# High-entropy materials for energy and electronic applications

**Simon Schweidler[1,9], Miriam Botros[1,9], Florian Strauss[1], Qingsong Wang[2,3], Yanjiao Ma[1], Leonardo Velasco[4], Gabriel Cadilha Marques[1], Abhishek Sarkar[1,5], Christian Kübel[1,5,6,7], Horst Hahn[1,5,8] ✉, Jasmin Aghassi-Hagmann[1] ✉, Torsten Brezesinski[1] ✉ & Ben Breitung[1] ✉**

High-entropy materials (HEMs) hold promise for a variety of applications because their properties can be readily tailored by selecting specific elements and altering stoichiometry. In this Perspective, we highlight the emerging potential of HEMs in energy and electronic applications. We place particular emphasis on (ionic and covalent) ceramics that have only emerged in powder form since 2015. Although the discovery of opportunities is in its early stages, we discuss a few case studies in which the use of HEMs has led to improved material properties and device performance. We also correlate features with the respective properties and identify topics and effects for future investigations. An overview of these intrinsic properties, such as cocktail effects, lattice distortions and compositional freedom, as well as a list of general attributes, is given and linked to changes in material characteristics.

[1]Institute of Nanotechnology, Karlsruhe Institute of Technology (KIT), Karlsruhe, Germany. [2]Department of Chemistry, University of Bayreuth, Bayreuth, Germany. [3]Bavarian Center for Battery Technology (BayBatt), University of Bayreuth, Bayreuth, Germany. [4]Universidad Nacional de Colombia sede de La Paz, Cesar, Colombia. [5]KIT-TUD Joint Laboratory Nanomaterials, Technical University of Darmstadt, Darmstadt, Germany. [6]Helmholtz-Institute Ulm (HIU) for Electrochemical Energy Storage, Karlsruhe Institute of Technology (KIT), Ulm, Germany. [7]Karlsruhe Nano Micro Facility (KNMFi), Karlsruhe Institute of Technology (KIT), Karlsruhe, Germany. [8]School of Sustainable Chemical, Biological and Materials Engineering, The University of Oklahoma, Norman, OK, USA. [9]These authors contributed equally: Simon Schweidler, Miriam Botros. ✉e-mail: horst.hahn@kit.edu; jasmin.aghassi@kit.edu; torsten.brezesinski@kit.edu; ben.breitung@kit.edu

## Introduction

As technology continues to advance and applications become more specialized, there is an increasing demand for materials with new functionalities and properties that satisfy specific requirements. Increasing the chemical complexity of materials beyond the current state of the art is one strategy that has been proposed to address this need and that has led to a new class of materials. These materials, called high-entropy materials (HEMs), are composed of many different elements in a single-phase crystal structure, opening up a vast chemical parameter space with virtually an infinite number of element combinations. This versatility allows compounds to be designed to meet specific needs and tailored to desired properties and applications, improving the quality and functionality of materials in a sustainable manner — for example by minimizing the concentration, or completely replacing scarce or toxic elements with more abundant and non-toxic ones.

Initial reports on multielement materials, specifically high-entropy alloys (HEAs), were published in 2004 (refs. 1,2). The approach was extended to high-entropy ceramics (HECs), with the first instances in powder form being high-entropy oxides (HEOs), introduced in 2015 (ref. 3). Since then, many other materials have been identified, and the term HEMs has been introduced to describe more broadly this new class of inorganic solids[4,5].

In HEMs, the variation in Gibbs free energy from the introduction of individual elements ($\Delta G_{mix}$) arises from alterations in enthalpy ($\Delta H_{mix}$, denoting the energy required to mix elements in a single-phase structure) and entropy ($\Delta S_{mix}$), following the equation $\Delta G_{mix} = \Delta H_{mix} - T\Delta S_{mix}$. $T\Delta S_{mix}$ can at times counterbalance $\Delta H_{mix}$, leading to a more negative $\Delta G$. The delicate interplay between $\Delta H_{mix}$ (typically positive) and $-T\Delta S_{mix}$ (typically negative) can result in what is known as 'entropy stabilization', wherein a single-phase structure becomes predominant at higher temperatures, whereas a multiphase material prevails at lower temperatures[6]. Entropy stabilization arises only when entropy becomes the key factor in the thermodynamic landscape and modulates structure and phase behaviour. Other entropy contributions can also play decisive roles in stabilizing certain phases (Supplementary Information). It should be noted that overcompensation does not necessarily lead to the formation of a single-phase material, as local energy landscape minima can impede the incorporation of elements (multicomponent phases are sometimes formed that include some but not all elements), and that it is also possible for certain thermodynamically unstable non-HEMs (for example $Bi_2Ti_2O_7$, which is thermodynamically unstable in the $Bi_2O_3$–$TiO_2$ phase diagram) to undergo transformation into a stable version by means of increased entropy[7]. A thorough description and/or analysis of the impact of entropy on thermodynamics and phase stability can be found elsewhere[8–10].

Several studies have recommended adopting the term 'high-entropy' for materials that show a configurational entropy ($S_{config}$) above a specific threshold (1.5 $R$, with $R$ representing the ideal gas constant), even if they do not necessarily demonstrate entropy stabilization. We suggest adhering to this terminology, as it helps to prevent avoidable confusion and provides a clear distinction between HEMs and conventional alloys or multicomponent materials that may not exhibit a high configurational entropy. The rationale behind this is explained in the Supplementary Information, along with a brief overview of existing naming approaches and an elaboration of the impacts of different types of entropy.

For calculating the total entropy of a solid, in addition to $S_{config}$, other contributions, such as vibrational, electronic or magnetic entropy, must be considered. Using finite-temperature ab initio methods, it was shown that although vibrational entropy ($S_{vib}$) can have a substantial effect, its absolute value alone does not always determine relative phase stabilities[11]. Instead, it is the variation in $S_{vib}$ among different phases that is relevant. At temperatures near 25 °C, for certain HEAs, this variation ranges within $1k_B$, underscoring its significance in determining their stability. Further investigations have also shown instances, where $S_{vib}$ decreases with an increasing number or diversity of elements, making its contribution to phase stabilities hard to predict[12] (Supplementary Fig. 1). We note that these calculations focused exclusively on HEAs. Given the substantial differences in chemical bonding, associated physical and mechanical properties, and general structures between alloys and ceramics, transferring the calculated results from metallic to ionic compounds is challenging. Nevertheless, considering the findings from these studies, it remains justifiable to regard $S_{config}$ as the primary component when additional elements are added while acknowledging the significance of other entropy types. Therefore, $S_{vib}$ should not be disregarded in ceramic systems.

The properties of HEMs can be modulated through elemental selection and composition (Box 1). The most important features that arise from a high configurational entropy are cocktail effects, (local) lattice distortions, high defect density, and improved stability of the crystal structure. A more detailed description can be found in Box 1. In addition, when seeking materials for a specific application, we advise considering not only single-phase structures, but also taking into account multiphase structures that may potentially meet the requirements. This approach offers endless opportunities to tailor properties to specific applications, making HEMs highly desirable for fields including energy and electronics. Nowadays, application-oriented research on HEMs as functional materials is focused on studying the properties that arise from the unique features of the high-entropy design concept, as entropy stabilization, as explained above, occurs only under certain energetic conditions and is often difficult to prove[8].

The high-entropy concept can be applied to any material that demonstrates a strong correlation between crystal structure and properties, which is true for most compounds used in electrochemical energy storage and conversion, electronics and optics, as well as many in other fields. The ability to substitute individual elements and adjust the stoichiometry of the material offers the opportunity to reduce the concentration of toxic or scarce elements while preserving the properties. Another factor that increases the variability and complexity of HEMs is the ability to incorporate elements in structural environments that they would not typically adopt (Fig. 1). However, altering the composition of materials may not always lead to the same or improved characteristics, and thus the advantages and challenges of high-entropy structures must be carefully considered (Box 1).

Typically, functionality can be enhanced through a systematic approach involving the modification of stoichiometry or composition. This enhanced functionality has been demonstrated in the tailoring of properties such as hardness of coatings[13], thermal conductivity[14], energy-storage density[15] or ionic conductivity[16], to name a few. Alhough this requires a large number of experiments owing to the vast number of possible element combinations, theoretical modelling and high-throughput screening techniques can help to limit the number of materials to be tested and speed up the research and development of HEMs. The introduction of the high-entropy concept in materials design has led to innovative approaches in developing advanced inorganic and hybrid organic–inorganic compounds[17] that have enabled

## Box 1

# Advantages and distinctive features of high-entropy materials

High-entropy materials (HEMs) are a class of materials characterized by the incorporation of a minimum of five distinct elements within a single-phase lattice structure. This elevates configurational entropy, a measure of entropy arising from the mixing of dissimilar elements, producing unique material properties. HEMs encompass various subtypes, with high-entropy alloys and high-entropy ceramics being the most prominent; the latter have a more complex arrangement, often comprising multiple sublattices including cationic and anionic sublattices. When evaluating configurational entropy, one must scrutinize these sublattices independently. The combination of dissimilar elements or ions, characterized by disparities in size, electronegativity and other factors, induces lattice distortions and intricate interelement interactions. This interplay initiates a cascade of electronic, physical, chemical and structural effects within the material (see the table).

The capacity to incorporate a diverse array of elements and to manipulate stoichiometries within HEMs offers an expansive chemical parameter space and an incalculable number of elemental permutations and resulting materials. Given that each composition can theoretically yield distinct properties, the potential applications of HEMs are, in principle, boundless. The ability to replace, introduce or remove elements offers virtually limitless opportunities for optimizing properties. Coupled with the controllable manipulation of high defect densities, this makes HEMs a valuable category of multifunctional materials for future applications.

However, the vast array of potential compositions makes it a formidable challenge to identify the best possible material for a given application. High-throughput synthesis and characterization techniques, along with theoretical calculations, become necessary to streamline the selection process and reduce the pool of promising materials to a manageable subset.

One of the key aspects of HEMs is the ability to tailor their properties and functionalities to suit specific applications, because of the high degree of control over composition, stoichiometry and defect structure. The resulting 'cocktail effects' can lead to altered states, depending on the degree of disorder present. In addition, lattice distortions may be induced by the introduction of ions of differing sizes, and structural stabilization can also occur. The interplay between cocktail effects and lattice distortions can engender distinctive conditions for the incorporation of ions within materials. These effects compel elements to adopt exotic structural environments that deviate from their typical configurations. The inclusion of CuO in a high-entropy rocksalt structure is a noteworthy case[3]. These alterations in both structural and electronic attributes modify the mechanical, electronic and electrochemical properties of materials. The extent of these changes is intricately intertwined with variations in the composition. Furthermore, the substitution of scarce and toxic elements with more sustainable counterparts is a focus of investigation in this domain, as it presents an avenue to improve the environmental and resource sustainability of materials. HEMs also exhibit an increased defect density, further contributing to their complexity and multifaceted nature.

| General attribute or properties | Advantages of high-entropy approach | Reason for improvements |
|---|---|---|
| Sustainability | Minimization of the concentration of scarce and/or toxic elements, replacing them with more abundant and sustainable elements | Cocktail effects |
| Tailoring | Alteration of the material properties by changing the composition, stoichiometry, etc. | Cocktail effects |
| Composition | Increasing the number of possible compositions, wide chemical parameter space | High-entropy composition (at least five elements of different stoichiometries in a single-phase structure) |
| Mechanical properties | Distortions through different ion sizes, electronegativities, defects, etc. leading to altered mechanical properties | Lattice distortion |
| Electrochemical properties | Inhibited phase transitions during charging and discharging, complex redox reactions of involved elements, changes in oxidation states, etc. | Cocktail effects, lattice distortion, structure stabilization |
| Electronic properties | Elements forced into exotic environments, band-structure changes, changes in oxidation states, etc. | Cocktail effects, lattice distortion, structure stabilization |
| Phase stabilization | Stabilization of phases otherwise inaccessible, overcoming solubility limits | Structure stabilization, cocktail effects |
| Vacancy and defect formation | Alteration of material properties through, for example, oxygen vacancies | High defect density |
| Surface modification | Uniform dispersion of elements leading to unique surface constitution | High-entropy composition (at least five elements of different stoichiometry in a single-phase structure) |

### Cocktail effects

The best-known effect is the 'cocktail effect', in which a mixture of elements or materials shows properties that cannot be attributed solely to any of its individual components. It arises from the complex interactions of the small units that make up the mixture, leading to unpredictable properties of the total system. If the composition or stoichiometry of an HEM is altered, the properties may vary strongly, owing to resulting changes in interactions. These changes can lead to modifications of the oxidation states or chemical environments of the incorporated elements[165]. Consequently, material properties may be tailored by selecting specific elements and modifying the stoichiometry. Although local interactions between the elements

*(continued from previous page)*
cannot be determined individually, the combined result is typically reflected in new global properties.

### Lattice distortions

Lattice distortions have an important role in shaping the properties of materials. Geometric lattice distortions arise when atoms or ions of different size, valence and/or electronegativity coexist within the same sublattice. Such distortions are proportional to the difference in atomic and/or ionic radii, with greater discrepancies yielding greater distortions. The distortion of the lattice directly affects the lattice energy and $\Delta H$, with the Madelung constant, a quantity determining the electrostatic potential of a crystal, changing on lowering the unit-cell symmetry via local atom and/or ion displacements. The distances between nearest and next-nearest neighbours no longer have fixed values but rather follow a distribution. Investigations into the effect of lattice distortion on interatomic forces in alloys have demonstrated that a 1% change in interatomic spacing can result in a force alteration of about 12%, a highly pronounced effect[166]. In comparison, a 10% change in interatomic spacing may lead to complete decomposition of the crystal structure. In the case of high-entroy alloys, such as the Cantor alloy FeCoNiCrMn, calculated lattice distortions resulting from the involvement of distinct elements were relatively small on average. Therefore, simulations based on the assumption of undistorted lattices are promising. However, local fluctuations may still reach 3% and, when combined with data on the impact of changes in spacing, may strongly affect the properties of materials[167].

### Structure stabilization

Entropy stabilization of the structure may occur when the $-T\Delta S$ term of the Gibbs–Helmholtz equation overcompensates the change in mixing enthalpy. Other types of structural stabilization also have a critical role in phase transitions, such as those that occur on ion insertion into battery materials. Also, beyond the solubility threshold for binary materials, phase stabilization effects have been observed, including the formation of structural types that are atypical under conventional conditions. These compositionally complex materials are often more stable than their less intricate counterparts. Although it may not be definitively concluded that such an HEM is entropy-stabilized, it is clear that favourable effects are at play, even if they cannot yet be fully explained mechanistically. The origins of these effects are likely to be as diverse as the domains in which stabilization is observed. It is unlikely that a single characteristic determines all observed effects; rather, many factors may collectively contribute to the observed structural stabilization.

the customization of materials structure and functionality, leading to unprecedented properties.

In this Perspective, we argue that HEMs have tremendous potential in fields such as energy storage, energy conversion and electronics (Table 1). We focus on promising ionic materials, including oxides, sulfides, carbides, nitrides, fluorides and metal–organic frameworks (MOFs). For several case studies, we relate the property changes associated with the high-entropy concept to device performance and material attributes. We also provide an overview of promising applications for HEMs in the fields of electronics and energy.

## Energy storage and conversion applications

### Cathode and anode materials for electrochemical energy storage

Improving electrochemical energy storage is crucial to the global transition to a greener and more sustainable future. In particular, the growing demand for next-generation batteries with superior energy and power densities and alternative mobile charge carriers (such as $Na^+$) has stimulated research into substitute materials.

The energy stored in batteries depends strongly on the active materials used in the cathode and anode. The cathode material is often a bottleneck for improving battery performance, as redox reactions at high potentials tend to trigger undesirable side reactions. To overcome this limitation, layered multicomponent materials, although not yet venturing into the high-entropy domain, offer desirable properties. Among them are layered oxides, such as $Li(Ni_{1-x-y}Co_xMn_y)O_2$, commonly referred to as NCM or NMC, which have garnered considerable attention as high-capacity cathodes. These materials are composed of layers of metal oxides intercalated by lithium (or other ions). This structural arrangement aids the intercalation and deintercalation of the ions during cycling, and thus NCMs offer better cycling performance than many alternative redox-active materials.

Introducing more elements into the layered oxides, and therefore nearing or reaching the high-entropy regime, can stabilize the structure with positive impacts on the electrochemical properties[18–22]. For example, the layered oxide $Na_{0.62}Mn_{0.67}Ni_{0.23}Cu_{0.05}Mg_{0.09-2y}Ti_yO_2$ allowed stable charging and discharging up to a rate of 10C for over 2,000 cycles[21]. The capacity could also be increased from about 30 mAh $g^{-1}$ after 500 cycles at 120 mA $g^{-1}$ for $Na_{0.62}Mn_{0.67}Ni_{0.37}O_2$ (low entropy) to 100 mAh $g^{-1}$ for $Na_{0.62}Mn_{0.67}Ni_{0.23}Cu_{0.05}Mg_{0.09-2y}Ti_yO_2$ (medium entropy), by increasing the number of incorporated elements and therefore increasing the configurational entropy. The mean voltage for Na-ion intercalation, which is reflected in the full-cell potential, was also higher than that of the low-entropy material, owing to increasing transition metal–oxygen (TM–O) bond ionicity, and resulted in improved energy density (~365 versus 340 Wh $kg^{-1}$)[22]. However, to accurately resolve the interplay between long-range order and local chemical disorder, and understand how structural conditions influence the electrochemical properties, comprehensive studies at the atomic level are needed. These studies are particularly important, as doping with many different elements, while staying well below 1.5 $R$, improves the cyclability by decreasing the volumetric strain in Ni-rich cathodes during cycling to 0.3%[19].

Although other electrode materials, such as conversion or insertion materials – which completely convert their structure or insert ions into a non-layered structure during the redox reaction, respectively – may deliver higher specific capacities, they are more likely to suffer from structural degradation over time and/or have poor reaction kinetics, which ultimately limit their performance. High-entropy oxides, sulfides and fluorides have garnered attention for their use in high-performance conversion-type electrodes. As an example, $(FeMnNiCoCr)S_2$ demonstrated a specific capacity of 150–200 mAh $g^{-1}$, an increase compared with $CoS_2$ and medium-entropy $(FeMnNiCo)S_2$[23–29]. This improvement is

attributed partly to favourable redox reactions and the formation of a stabilizing matrix[26,30]. Similarly, (CoCuMgNiZn)O has enhanced cycling stability, characterized by improved capacity retention, in comparison to conventional metal oxide anodes. In a conventional conversion battery, the active material undergoes complex transformations during both charging and discharging, necessitating the complete rebuilding of the crystal structure with each cycle. Additionally, the generally low electrical conductivity of metal oxides hampers electron and ion transport within the material, thereby decelerating kinetics. By contrast, (CoCuMgNiZn)O does not fully convert into metals and $Li_2O$. Instead, certain elements, notably Mg, retain their positions within the parent structure, forming an MgO (rocksalt crystal structure) matrix. This matrix aids the reintegration of metal species during delithiation, which in turn helps to improve material stability throughout cycling and reduce the degradation due to stress and strain associated with 'conventional' conversion reactions (Fig. 2). Furthermore, complex interactions (cocktail effects) emerge among the constituent elements. During the conversion process, Co, Ni and Cu alloy together, whereas Zn reacts further with Li. Simultaneously, Mg persists as a rocksalt MgO matrix, featuring inclusions of $Li_xO$ species. On delithiation, the CoNiCu alloy does not fully revert back to metal oxides; instead, Co and Zn reintegrate into the rocksalt MgO matrix, resulting in a $(Co_{0.5}MgZn)O$ lattice. A $Co_{0.5}NiCu$ alloy forms a 3D network that extends throughout the entire particle that the material is composed of. This conductive alloy, combined with the stabilizing matrix, greatly improves electron transport within the material, and explains why eliminating certain elements, such as Co, results in the active material's failure. It underscores the pivotal role played by the combination of elements and their interplay in enhancing cycling stability and kinetics in HEOs. The performance of the high-entropy (CoCuMgNiZn)O, encompassing all five elements, was also benchmarked against all possible combinations of its medium-entropy counterparts, which consist of the same four elements with one systematically omitted[26]. Although the medium-entropy oxides behaved like conventional conversion-type materials and exhibited high capacity but low reversibility, the HEO, despite delivering slightly lower initial capacities, displayed exceptional endurance, maintaining a specific capacity around 600 mAh $g^{-1}$ for over 300 cycles[30].

Practical obstacles, notably the relatively high mean lithiation voltage and the pronounced voltage hysteresis, which result in low energy densities and efficiencies, continue to impede the use of any conversion-type electrode. The lithiation voltage represents an intrinsic property that depends on the elements and their oxidation states. By contrast, the hysteresis predominantly arises from kinetic challenges, giving rise to overpotentials. The prospect of surmounting these limitations, perhaps by augmenting both partial electronic and ionic conductivity during this process, warrants further research. Regardless, the stable high-entropy anodes mentioned above represent an important step towards the development of high-capacity electrode materials with improved performance.

Cation-disordered rocksalt (referred to as DRX) compounds are another promising class of next-generation cathodes. In such

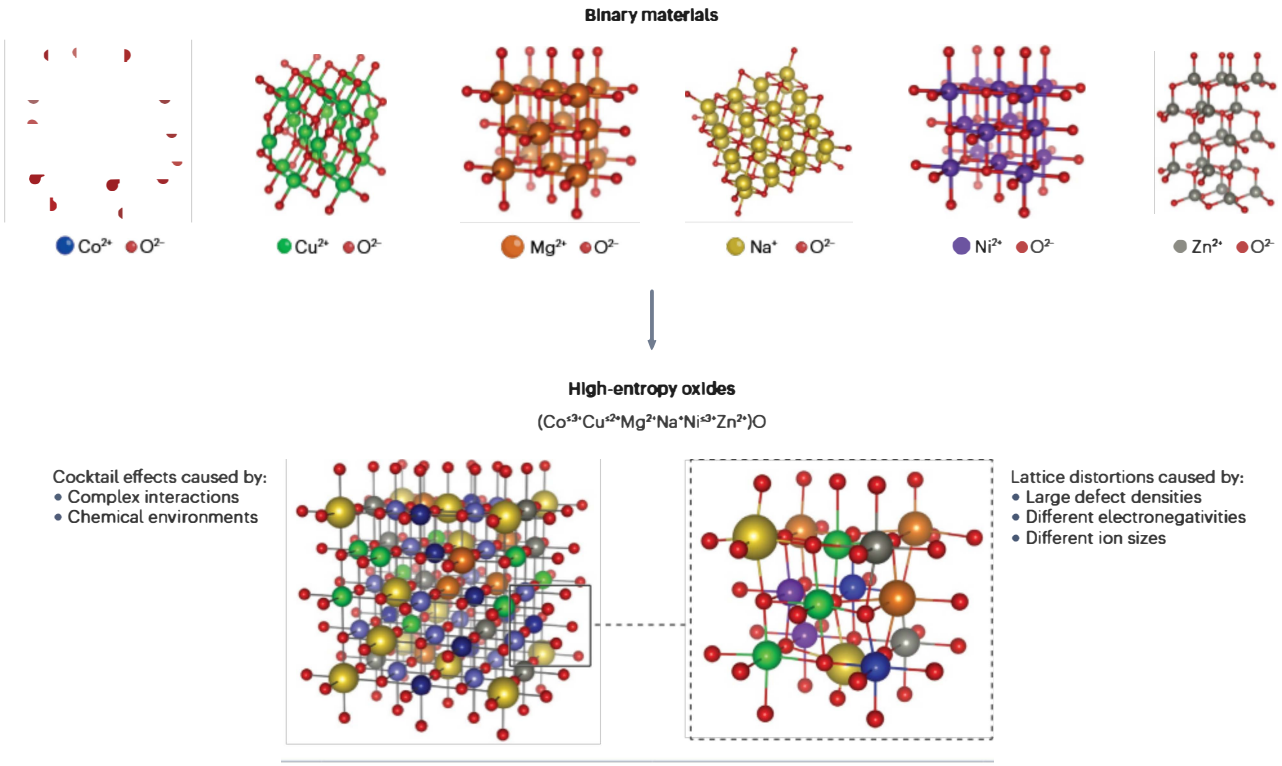


**Fig. 1 | The transformation of binary materials (simple oxides) into a high-entropy material.** Cocktail effects describe the feature that a mixture of elements often leads to greatly altered properties as compared with the binary materials, owing to complex interactions between the incorporated elements. Changes in chemical environment, crystal structure (including lattice distortions) and oxidation state have a strong effect on the material properties, as explained elsewhere[165].

**Table 1 | Overview of achieved property transformations for applications in energy storage, energy conversion and electronics**

| Application | Desirable property | Proposed reasons for improvement |
|---|---|---|
| **Energy storage** | | |
| Cathode material | Increased capacity | Lattice distortion leading to lower short-range order opens pathways for diffusion |
| | Structural stability | Increased stability of the crystal structure helping to suppress phase transformations during cycling, counteracting degradation |
| Anode material | Stable cycling performance | Cocktail effects resulting in the formation of a 3D alloy network through the particle, leading to improved conductivity and kinetics |
| | Structural stability | Formation of a matrix stabilizing the structure during the electrochemical reactions |
| Ionic conductor | Low activation energy for conduction | Cocktail effects |
| | | Lattice distortion altering the structure and energy barrier within the material |
| | Avoiding the use of scarce or toxic elements | Cocktail effects |
| | | Tailoring leading to altered compositions while still performing well |
| **Electrocatalysis** | | |
| | Improved efficiency | Cocktail effects leading to changes in electronic structure at the surface of the catalyst |
| | | Tailoring leading to surfaces with specific elements in a desired structure |
| | Long-term and thermal stability | Structure is more robust and less sensitive to corrosion |
| **Dielectrics** | | |
| | Change in dielectric constant | Tailoring of elements |
| | | Lattice distortion enhancing the polarization capabilities by affecting the distribution of charges within the lattice |
| **Thermoelectrics** | | |
| | Low thermal conductivity | Lattice distortion inducing phonon scattering and reducing phonon-based heat transfer |
| **Semiconductors** | | |
| | Semiconducting behaviour | Tailoring of elements leads to improved mobility |
| **Magnetoelectrics** | | |
| | Modulation of properties | Lattice distortion leading to different ligand–metal–ligand bond angles, affecting exchange interactions |

materials, short-range order can hinder diffusion pathways by limiting long-range lithium transport and negatively affect cyclability. By changing the composition to obtain a high-entropy oxyfluoride, lithium diffusivity has been successfully improved, aiding the activation of the material[31,32]. Incorporating elements of varying sizes induces lattice distortions, resulting in a reduction of short-range order in the crystal structure[32]. This mechanism effectively creates additional accessible pathways, thereby substantially enhancing the charge-storage properties. For instance, the introduction of six transition metal species into a material that initially contained only two led to an increase in specific capacity from about 200 to 300 mAh $g^{-1}$. In addition to improved kinetics, the chemical flexibility and the ability to eliminate toxic and expensive elements like cobalt without compromising energy density on a cell level make DRX materials (such as high-entropy oxyfluorides) valuable alternatives to current cathode materials[31,32].

In addition, high-entropy metal–organic frameworks (MOFs), specifically Prussian blue analogues (PBAs), show improved performance over their low-entropy counterparts when used as insertion cathode materials in batteries[33,34]. For Li–S batteries, the specific capacity was increased from 340 mAh $g^{-1}$ for low-entropy PBAs to 570 mAh $g^{-1}$ for high-entropy PBAs as sulfur hosts after 200 cycles, whereas for Na-ion batteries in rate performance tests, an increase from 47 mAh $g^{-1}$ for low-entropy PBAs to 79 mAh $g^{-1}$ for high-entropy PBAs was observed at 1 A $g^{-1}$ (refs. 33,35). The enhanced performance can probably be attributed to the suppression of phase transitions during sodiation and desodiation processes in these materials. Although PBAs with only one or a few incorporated elements (that is, low- or medium-entropy PBAs) show a transition from cubic to tetragonal structure and back during cycling, high-entropy PBAs maintain the cubic structure throughout the entire cycle, avoiding any phase changes and severe volume variations. Consequently, high-entropy MOFs can operate with minimal strain, thus experiencing little to no structural alteration. This minimal structural change aids in preventing chemomechanical degradation and capacity fading.

Overall, key differences between low- and high-entropy materials, which substantially affect their electrochemical properties, arise from features such as cocktail effects and lattice distortions. These differences include variations in electronic conditions, reduced energies of formation in specific states, distortions leading to altered lattice parameters, improved ion diffusivity and modified mechanical properties, among others. The precise mechanisms underpinning the structural stabilization, as explained above, are poorly understood. However, a general stabilization during cycling has been observed

in various high-entropy structures. Examples include layered HEOs for sodium storage, high-entropy sulfides and oxides for conversion reactions, and even high-entropy doping, in which introducing minor concentrations of different elements into a Li-intercalation material substantially enhances stability during cycling[35,36]. It is likely that various effects play a pivotal role in each of these materials. Although different materials have been tested, the impact of the initial structure and composition on the long-term stability has not yet been clarified and requires further investigations or theoretical consideration. Another promising area of research is the study of the solid electrolyte interphase (SEI) formation and composition. Advances in cryo-transmission electron microscopy (cryo-TEM) and lithium quantification by titration offer new possibilities for investigating the SEI, which forms on the free surface of active electrode materials during cycling and strongly affects the charge-transfer kinetics. Additionally, the use of HEAs for Li-storage by alloying reaction remains largely unexplored, with only a few reports existing in the literature. Future research in this area could provide insights into the potential of HEAs as electrode materials for high-performance batteries[37,38].

## Superionic conductors for semi- or all-solid-state batteries

Bulk-type solid-state batteries (SSBs) differ from conventional batteries in using superionic solid electrolytes instead of liquid electrolytes. In this design, the solid electrolyte serves as both the ion conductor and separator while offering larger operating voltage windows (depending on the type of solid electrolyte used). These characteristics position SSBs as potential candidates for delivering superior power and energy densities with greater safety, particularly through the reduction of

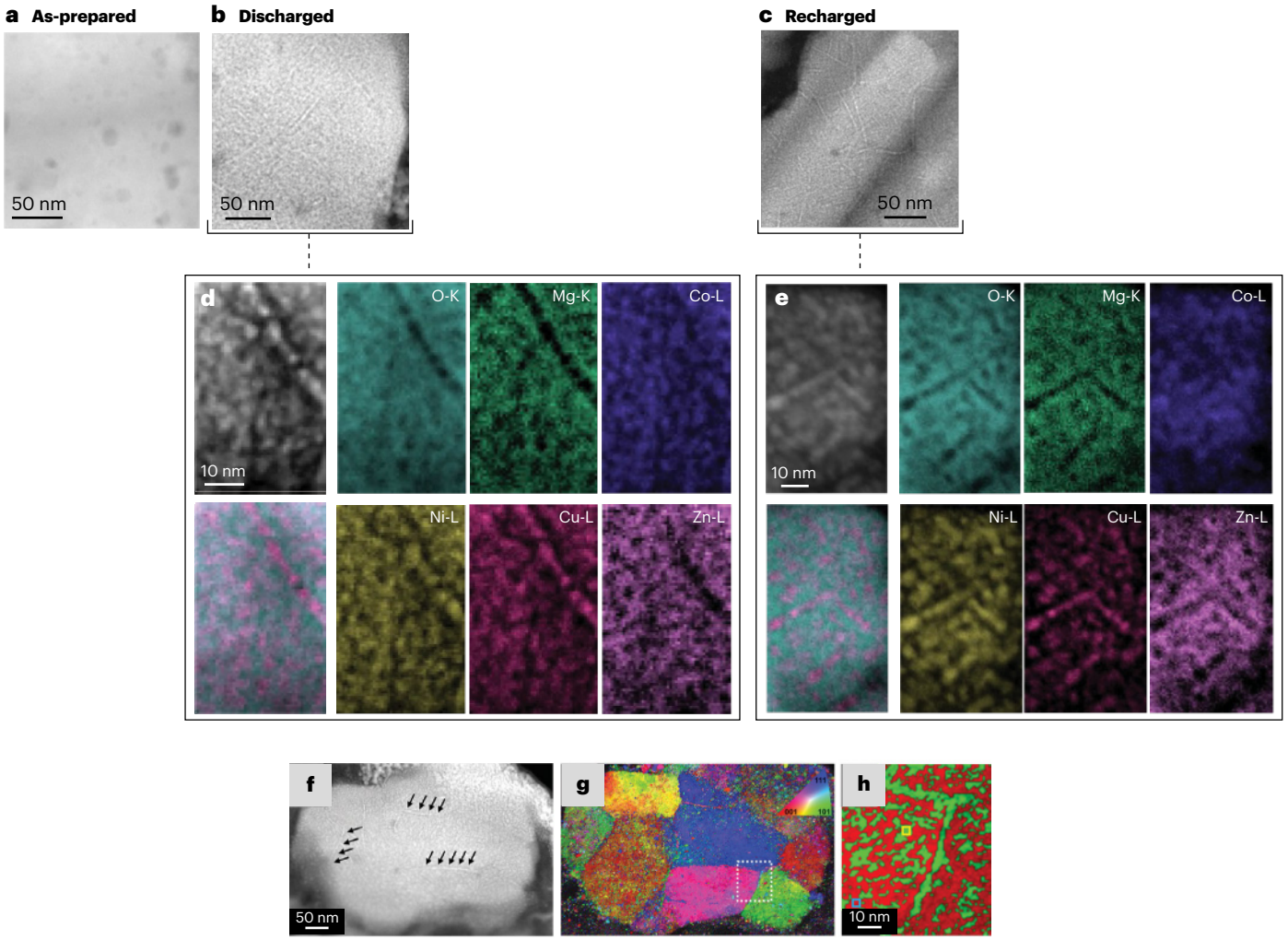


**Fig. 2 | Cocktail effects during the conversion reaction of the (CoCuMgNiZn)O anode. a**–**c**, Scanning transmission electron microscopy (STEM) analysis of the microstructural evolution of the material at distinct stages: representative high-angle annular dark-field STEM (HAADF-STEM) images of the as-prepared (panel **a**), discharged (lithiated; panel **b**) and recharged (delithiated; panel **c**) state. **d**,**e**, STEM–electron energy loss spectroscopy (STEM-EELS) elemental maps of the discharged (panel **d**) and recharged (panel **e**) state. The co-localization of the elements shows alloy formation of Ni, Cu and Co in the discharged state and the continued presence of MgO. Similarly, in the recharged state Ni, Cu and partially Co are alloyed while Mg and Zn are present as oxide. **f**, HAADF-STEM overview image of a particle with arrows denoting enhanced alloy formation at grain boundaries. **g**, Corresponding 4D-STEM-based orientation map showing the local grain orientation in the particle. **h**, Representative phase map of the region marked by the white box in panel **g**, where green indicates regions dominated by the metallic alloy and red represents regions dominated by the metal oxide. Adapted from ref. 30, CC BY 4.0.

leakage, thermal runaway and dendrite formation. However, SSBs still face major challenges, including high manufacturing costs and issues associated with cycling performance and stability. The issues encompass complex chemical reactions occurring at the electrode–solid electrolyte interface, the electrochemical and mechanical stability of the solid electrolyte during cycling, and sensitivity to temperature fluctuations, among others. Therefore, superionic and electrochemically stable solid electrolytes are of paramount importance for the development of advanced SSBs.

High-entropy conductors enable tailorable (electro)chemical and mechanical properties through compositional design, and thus could be used to improve the stability of SSBs. In addition, in these materials, ionic conductivity can be increased by improving ion transport (diffusion) through the alteration of the crystal structure via substitution or doping with iso- or aliovalent ions. By integrating various ions into the host structure, lattice distortions can be used to tailor the energy landscape, potentially resulting in decreased activation energies for conduction. High-entropy materials can show high ion diffusivity at room temperature due to overlapping site-energy distributions induced by local structural distortions.

So far, the high-entropy concept has been applied to four material classes, namely the rocksalt[16,39–41], NASICON (Na superionic conductor)[42], garnet[42–45] and argyrodite structures[46,47]. The first three are oxide-based ceramics, whereas argyrodites refer to thiophosphates. In the garnet-type material $Li_7La_3Zr_2O_{12}$, $La^{3+}$ and $Zr^{4+}$ have been successfully substituted with various cations but without notable increase in ionic conductivity or decrease in activation energy for conduction[42,43]. Similarly, in argyrodites ($Li_6PS_5X$, with X = Cl, Br, I), both anion (S and X sites) and cation (P site) were substituted (with S, Se, Cl, Br, I, Si, Ge or Sb on the respective sites), but no major improvements in conductivity over other (single-substituted) lithium argyrodites were achieved[46,47]. Nevertheless, low activation energies, stemming from an optimized energy landscape for charge transport, seem to be a key feature of such HEMs and should motivate further studies in this area. These low activation energies may result from overlapping energy distributions on the lithium sites or from occupation of interstitial or transition sites, where an optimal degree of distortion is needed to boost ionic conductivity. The activation energy is also affected by a softened lattice resulting from the multielement composition (vibrational entropy contributions). The activation energy for conduction was decreased to 0.22 eV for $Li_{6.5}(Ge_{0.5}P_{0.5})(S_{2.5}Se_{2.5})(Cl_{0.33}Br_{0.33}I_{0.33})$[47].

In oxide Li-ion conductors, a high $\Delta S_{config}$ has been achieved by mixing only the cations without addressing the anions. Initially, this was demonstrated for rocksalt materials, such as $(MgCoNiCuZn)_{1-x-y}Ga_yA_xO$ (A = Li, Na, K), with room-temperature conductivities reaching $10^{-3}$ and $5 \times 10^{-6}$ S cm$^{-1}$ for lithium and sodium, respectively[16]. However, because these materials lack intrinsic lithium diffusion pathways, the detailed transport mechanism is still unclear and is speculated to be aided by oxygen-vacancy formation. An increased electronic contribution to the conductivity has also been put forward, which would render the material unsuitable for SSB applications, as the primary mode of conduction should be ionic[48].

Much more work is required to validate the benefit of using high-entropy solid electrolytes and gain a better understanding of the impact of the crystal structure and lattice distortions on ion mobility in HEMs. This validation is a non-trivial task, calling for advanced analytical techniques capable of probing short- and long-range structural properties and computational methods. Apart from that, it is challenging to separate the influence of configurational entropy and correlated lattice dynamics (phonon broadening) on ion diffusion. Investigating ion-conducting materials with different crystal structures would be beneficial in this regard. We believe that the high-entropy concept offers new opportunities for discoveries even beyond Li-ion chemistries.

## Electrocatalysis and energy conversion

Energy conversion is another electrochemical process that is essential for the hydrogen economy. Electrolysis-driven water splitting is a promising approach for producing green hydrogen, which can be used efficiently and on a large scale as a fuel for energy conversion, transport and storage[49]. However, the efficiency of electrochemical water splitting is limited by the kinetically slow gas evolution processes occurring at the electrodes. The oxygen evolution reaction (OER) is the primary bottleneck, as the slow electron-transfer kinetics make it challenging to form certain (surface) transition states, leading to overvoltages that negatively affect energy efficiency. Therefore, there is a need to develop catalysts with improved charge-transfer kinetics and surface transition states. Currently, the most efficient catalysts for the OER are based on noble metals, examples being iridium (Ir), iridium dioxide ($IrO_2$), ruthenium (Ru) and ruthenium dioxide ($RuO_2$), but these are not suitable for large-scale industrial applications because of their scarcity and high cost[50–52]. Consequently, there is a growing interest in developing new catalysts made from abundant (low-cost) elements. The challenge is to design catalysts that not only show excellent activity but also withstand the highly oxidizing and reducing conditions present during electrochemical water splitting. Ideally, they should also exhibit mixed ionic/electronic conductivity to aid charge transfer and should not segregate during operation[53]. Both metallic and non-metallic (ceramic) HEMs have been investigated for their potential as advanced catalysts in various electrochemical processes[54,55], including alcohol oxidation[56,57], thermocatalysis (CO oxidation, $NH_3$ oxidation and decomposition)[58–60] and electrocatalysis (OER, oxygen reduction reaction (ORR), hydrogen evolution reaction (HER) and $CO_2$ reduction reaction)[61–66].

Given that most catalytic reactions occur at the surface, the surface composition plays a crucial role in these applications. Through the uniform distribution of various elements in the bulk and the surface of the materials, high-entropy catalysts offer a distinctive surface structure, with each element serving as an individual catalytic centre. Furthermore, the ability to customize catalytic sites, control the defect structure, induce lattice distortions to lower system energy and tailor the electronic structure, such as through modified Jahn–Teller effects (a spontaneous symmetry reduction to minimize overall energy), distinguishes high-entropy catalysts from conventional single- or multicomponent catalysts[55]. For reasons mentioned above, many HEMs show substantially higher activity than conventional catalysts[66,67]. For example, the high-entropy sulfide $FeNiCoCrMnS_2$ revealed an overpotential of only 246 mV at 100 mA cm$^{-2}$ (for comparison, $RuO_2$ as a state-of-the-art catalyst showed 346 mV at 100 mA cm$^{-2}$) and showed stability over 12,000 cycles at 500 mA cm$^{-2}$ (ref. 66). Overall, HEMs have great potential as high-efficiency catalysts for electrochemical water splitting[68]. However, further research is needed to address the scalability and stability of HEMs under harsh conditions, as the existing synthesis methods are difficult to upscale.

Spinel- and perovskite-type oxides are a fascinating class of ceramic materials because of their dual cation sites and oxygen non-stoichiometry[63,65,69–72]. These characteristics allow electronic

and physiochemical properties to be customized, making them suitable for specific catalytic applications through the application of the high-entropy concept on many different lattice sites. For instance, perovskite materials such as $La_{0.7}Sr_{0.3}(CoCrFeMnNi)O_3$ showed high catalytic activity, good durability and noteworthy thermal and chemical stability (no signs of performance degradation after 50 h while testing at 10 mA $cm^{-2}$). Meanwhile, spinel-type $(CrMnFeCoNi)_3O_4$ displayed a Tafel slope of 49.1 mV $dec^{-1}$ (describing the kinetics of the catalytic reaction), lower than that of the reference material $IrO_2$, which registers at 52.9 mV $dec^{-1}$ (refs. 73,74).

The complex chemical environment of HEMs is well suited to the formation of multiple metastable active sites that can adsorb transient reactants at different energies[75–77]. Seawater is the primary source of water on Earth, comprising 95% of the total[78–81], which has led to decades of studies on seawater electrodes for water splitting[82]. The salinity of seawater, with about 3.5 wt% NaCl (pH ≈ 8), presents a challenge, as it triggers a competition between $Cl^-$ and $O^{2-}$ during redox processes. The identification of catalysts that are capable of suppressing the competing detrimental reaction would be highly attractive[83–86]. Potential strategies include changing the electronic structure of the catalyst or engineering its surface with many different elements and making use of its increased stability. Furthermore, a finely tuned and efficient high-entropy catalyst for water splitting under high pressure could improve the energy efficiency of producing, transporting and using compressed hydrogen gas (500–700 bar) as a renewable energy carrier.

Hydrogen adsorption and CO diffusion loss are challenging issues for traditional catalysts. When hydrogen fails to be adsorbed effectively at the surface or when CO rapidly diffuses away from the catalytic centres, the overall process becomes markedly inefficient. HEMs can overcome these obstacles by increasing selectivity (controlling cascade reactions) and optimizing microstructure[87].

Energy conversion devices, such as solid-oxide cells and fuel cells, and Zn–air batteries, which require high catalytic activity, thermal stability and durability, are good application targets for HEMs[23,88]. HEMs can also be easily integrated into ceramic micro solid-oxide cells by using thin-film technologies[89]. HEAs and HEOs can be combined by introducing alloys into an oxide matrix[90–92]. Doing so allows OER and ORR to be performed at different potentials, catalysed by the respective alloy or oxide, and still achieving improved activity and high stability. HEMs may also offer similar properties for oxygen conductors and/or proton conductors by reducing energy barriers through lattice distortions[42]. However, there are only a few reports available on high-entropy electrolytes for energy conversion devices, and it remains to be seen whether this new class of materials can outperform state-of-the-art electrolytes[93].

Energy conversion applications, including solid-oxide cells, $CO_2$ reduction and water splitting[24], benefit strongly from material durability and high catalytic activity. However, the successful integration of HEMs into electrochemical devices requires a deeper understanding of the interplay between lattice distortions, electronic structure, defect formation mechanisms and intrinsic properties (such as ionic conductivity) while taking advantage of their versatility for achieving desired compositions. A fundamental understanding of these processes will further advance application-oriented materials research and development.

Overall, different effects can emerge from the high-entropy concept to have an impact on energy storage and conversion applications (Fig. 3).

## Electronic applications

### Dielectrics

Dielectric materials are essential for various electronic applications, particularly in devices such as capacitors and transistors[94]. Different components require specific properties; for example, for capacitive energy storage, high dielectric constant and low dielectric loss are needed, whereas information storage requires minimal leakage currents to avoid information loss. High-permittivity materials (high-$\kappa$, typically defined as materials with a greater dielectric constant than that of $SiO_2$ with ~3.9) are necessary for transistors to operate, whereas low-$\kappa$ materials are advantageous for reducing parasitic capacitances in the backend.

The high-entropy approach offers a means to customize the characteristics of dielectric materials, notably by influencing the dielectric constant. By introducing lattice distortions and strain in multicomponent materials, the polarization behaviour can be tuned. Oxygen vacancies, which are often present in HEMs, can also substantially affect the dielectric properties by changing the polarization behaviour[95,96]. High-$\kappa$ HEMs, such as $(La_{0.2}Li_{0.2}Ba_{0.2}Sr_{0.2}Ca_{0.2})Nb_2O_{6-\delta}$, a ceramic with a dielectric constant of $1.1 \times 10^6$ at 100 Hz (almost 1,290 times as large as for $(BaSrCa)Nb_2O_6$ ceramics), have been reported. However, the dielectric constant was found to be highly dependent on frequency[97]. Strong dielectric relaxation effects, which refer to the response of a material to an alternating electric field and the associated delay, have been observed and attributed to the presence of oxygen vacancies. At frequencies higher than $10^3$ Hz, the dielectric constant saturates several orders of magnitude below the reported value. Frequency dependency is an issue seen not only in high-entropy dielectrics but also in non-high-entropy materials. Other high-entropy compositions, such as $[(Ce_{0.5}K_{0.5})(Bi_{0.5}Na_{0.5})_{0.25}Ba_{0.25}Sr_{0.25}Ca_{0.25}]_{1-x}TiO_3$, exhibit a stable (large) dielectric constant even at very high frequencies (with $\kappa = 535$ between $10^2$ Hz and $10^9$ Hz)[98].

Most of the HEO dielectrics reported in the literature are actively used for capacitive energy-storage applications, for which careful selection of the constituent elements allows targeted design of material properties[99–102]. Another important feature is the possibility of overcoming solubility limits. For example, a pyrochlore $Bi_2Ti_2O_7$-based dielectric of nominal composition $(Bi_{3.25}La_{0.75})(Ti_{3-3x}Zr_xHf_xSn_x)O_{12}$ was capable of achieving an excellent energy-storage density of 182 J $cm^{-3}$ at 6.35 MV $cm^{-1}$. It also showed over 90% efficiency at 5 MV $cm^{-1}$ and maintained good thermal stability[7]. $Bi_2Ti_2O_7$ is thermodynamically unstable, but its high-entropy counterpart can be thermodynamically stabilized, avoiding decomposition and therefore overcoming solubility limits.

High permittivity, high breakdown voltage and good interfacial properties are beneficial for the performance of gate insulation materials[103]. For emerging technologies such as printed electronics, replacing traditional high-$\kappa$ dielectrics with an electrolyte improves the interface with the semiconductor, which can greatly reduce the supply voltage requirements[104,105]. A similar approach can be taken with HEMs, where interfacial properties and dielectric constant are tailored to increase the current density of the transistor while reducing the voltage requirements.

As another example, ferroelectric dielectrics can exhibit extraordinarily large dielectric constants (up to 15,000 for $BaTiO_3$) due to temperature-dependent spontaneous domain depolarization, particularly in a narrow temperature range that approaches the material's Curie temperature. The downside is that the dielectric constant depends on the strength of the electric field; when spontaneous polarization is not feasible, the permittivity drops to values similar to those of classical dielectrics (for example 20–70 for $TiO_2$). Overall, it remains

to be seen whether the high-entropy concept can help in designing materials that can be used in a wider temperature range or at stronger electric fields. Nevertheless, this design strategy is clearly beneficial for certain materials[106].

### Thermoelectrics

Thermoelectric materials use the Seebeck effect to generate a voltage in response to a temperature gradient across the material. As such, they hold promise for environmentally conscious applications, such as

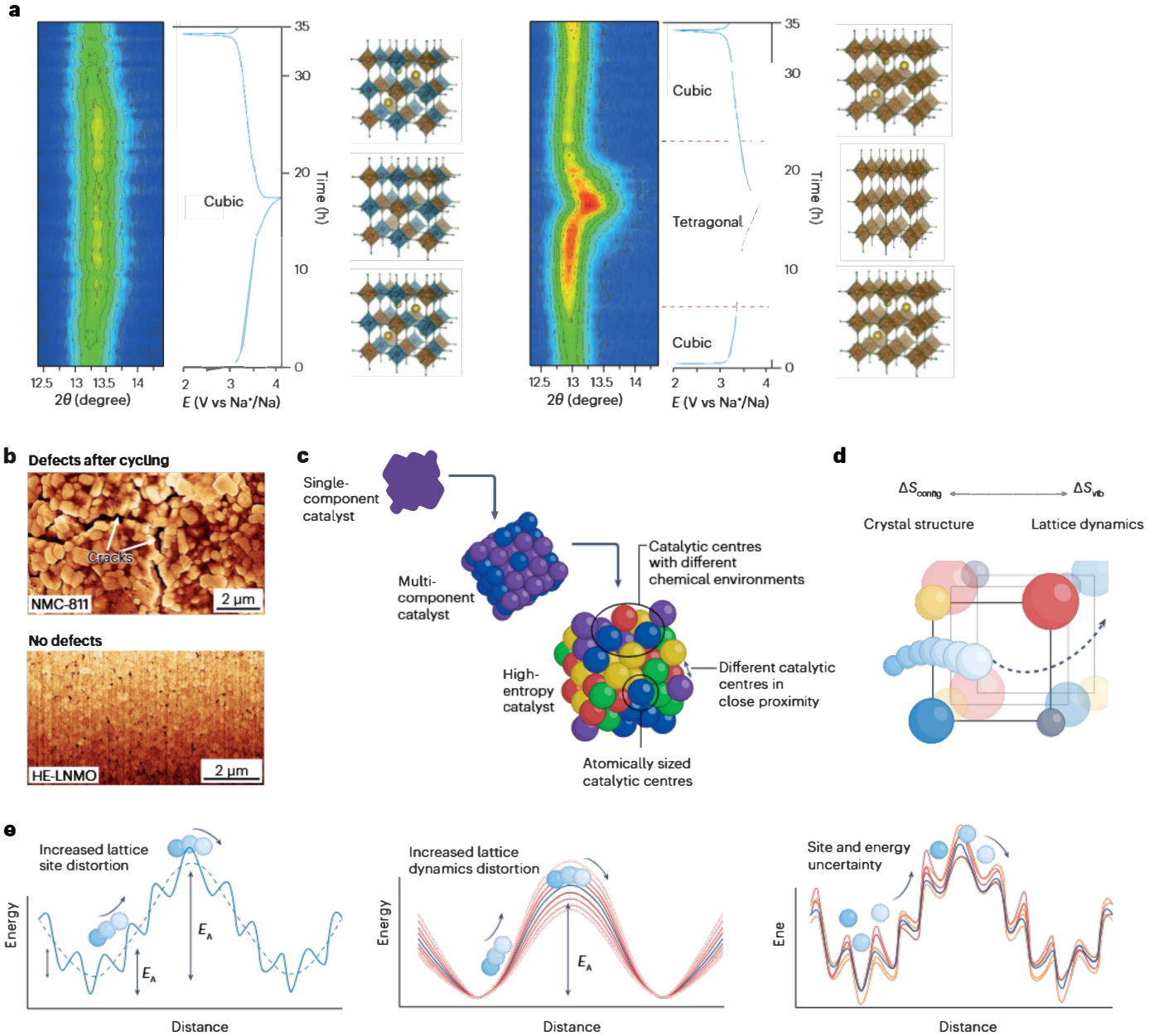


**Fig. 3 | Different effects emerging from the high-entropy concept and how they affect energy storage and conversion applications. a**, Structural stabilization of high-entropy metal–organic frameworks during sodiation and desodiation. Unlike the high-entropy material (left part), the low-entropy counterpart (right part) undergoes a phase transition from cubic to tetragonal, resulting in structural degradation. **b**, High-entropy doping severely reduces internal stress and/or strain build-up during battery operation, leading to reduced particle fracture in state-of-the-art cathode (NMC, $Li(Ni_xMn_yCo_z)O_2$; LMNO, $Li(Ni_xMn_y)O_2$) materials. **c**, Evolution from single-component to high-entropy catalysis. High-entropy catalysts benefit from a unique surface structure resulting from the uniform distribution of different elements that serve as distinct catalytic centres. **d**, Configurational entropy meets solid electrolytes. Scheme of how structural disorder affects the configurational entropy ($\Delta S_{config}$) and the vibrational entropy ($\Delta S_{vib}$). **e**, Structural disorder may induce favourable energy landscapes for ion transport with various interstitial sites (transition states), ultimately leading to a decrease in activation energy ($E_A$) for ion conduction (left part). Lattice dynamics are also affected, meaning that $E_A$ can be increased or decreased depending on the (local) lattice hardening or softening, respectively, which is reflected in $\Delta S_{vib}$ (middle part). The effect of the two entropy contributions combined (right part). Part **b** reprinted from ref. 19, Springer Nature Limited.

waste heat recovery or electricity generation from geothermal sources. However, they usually require toxic and costly elements, and their use has been limited by low conversion efficiency. The thermoelectric efficiency $zT$ can be calculated as:

$$zT = \frac{S^2\sigma T}{\kappa},$$

where $S$ represents the Seebeck coefficient, $\sigma$ the electrical conductivity, $T$ the temperature and $\kappa$ the thermal conductivity. In HEMs, disorder has a direct impact on thermal conductivity. Increased disorder and consequently lattice distortions disrupt the regular phonon vibrations that are primarily responsible for heat conduction by introducing phonon scattering centres[14,107–112]. Simultaneously, an increase in $\Delta S_{config}$ can increase solubility limits and reduce electron scattering processes by eliminating phase boundaries in systems that would otherwise form multiple phases, thereby improving electronic conductivity[113,114]. Although the inclusion of both strategies in a single material is difficult, this technique allows 'high' electronic conductivity to be coupled with low thermal conductivity, a prerequisite for high-performance thermoelectrics[115,116]. This behaviour can be found mostly in semiconductors, as they combine low electrical conductivity with high thermal conductivity[117].

Studies aiming to use HEMs for thermoelectrics have already been performed, with notable results. For example, a high-entropy chalcogenide, $Pb_{0.935}Na_{0.025}Cd_{0.04}Se_{0.5}S_{0.25}Te_{0.25}$, was used to construct a segmented thermoelectric module. This module achieved a high conversion efficiency of 12% at $\Delta T = 506$ K, which is among the highest reported values for thermoelectric systems[113]. This value was attained by systematic (and incremental) adjustment of the composition until an optimized configuration was reached.

Overall, the combination of chemical complexity and compositional disorder with the relatively high electrical conductivity of semiconductors renders HEMs a promising class of materials for next-generation thermoelectric applications[118–120]. The opportunity presented by the substantial effect of multielement substitution, which reduces thermal conductivity through local lattice distortions (scattering of heat-transferring phonons), makes the development of advanced thermoelectrics feasible.

### Semiconductors

Efficient semiconductors are important for the proper functioning of transistors, which form the fundamental unit of any electrical circuit. Carrier mobility and concentration are often affected by defects in the crystal structure, lattice distortions, and grain or phase boundaries. Although phase boundaries can be circumvented through the stabilization of otherwise thermodynamically unstable phases, for example by using entropy stabilization, the associated inherent lattice distortions can pose an important obstacle to fabricating high-mobility semiconductors, as they can act as electron-scattering centres[121,122]. Because HEMs naturally have lattice distortions due to the large number of elements in the crystal lattice, it is challenging to obtain high-entropy semiconductors with the desired performance. Nevertheless, efforts are underway to develop high-entropy semiconductors capable of undergoing, for example, temperature-dependent structural changes, affecting their band structure[123–126].

Beyond electronic conductivity, other parameters such as the threshold voltage, on/off current and durability also have a crucial role in electronic devices such as transistors. In complementary metal–oxide–semiconductor (CMOS) technologies, n- and p-type semiconductors with similar performance are preferable for circuit architectures. However, p-type semiconductors are often constrained by mobility limitations, which can only be overcome through expensive stress engineering methods. In these cases, the lattices are subjected to strain, for example by epitaxial growth on materials with slightly differing lattice parameters, and can show improved electron or hole conductivities. As this strain exists inherently in HEMs owing to the different sizes of the incorporated ions, strategies to exploit that could be very promising. HEMs can be tailored to achieve the desired properties or broaden the chemical parameter space for the selection of materials that would otherwise be unavailable because of solubility limitations[101].

### Magnetoelectrics

Magnetoelectric materials, in which magnetic and electrical properties are coupled, are rapidly emerging as promising candidates for many opportunities in the electronics industry. For example, electronic properties can be precisely controlled by a magnetic field, while magnetic properties can be tuned by an electric field. In metal oxides, the fundamental magnetic and electronic interactions are predominantly governed by the indirect exchange coupling of neighbouring cations through the intermediary oxygen. Therefore, the types of metal cations, their oxidation and spin states, and the characteristics of the metal–oxygen–metal (M–O–M) bonds are vital factors that influence the material properties. Additionally, the magneto-electronic ground state of the material depends on the crystallographic structure.

HEOs manifest additional phenomena that are believed to arise from their unique materials design. They can show a gradual magnetic transition that, accompanied by an anomalous change in heat capacity around the transition temperature, is thought to result from a distribution of bond angles and may lead to different exchange interactions[127–129]. Unlike conventional oxides, the presence of different cations results in a broad distribution of M–O–M bond angles while retaining long-range magnetic ordering[128–132]. Apart from that, HEOs have remarkably similar magneto-electronic properties to their isostructural, low-entropy counterparts[127]. For instance, transition metal-based rocksalts[128] and rare-earth/transition metal-based perovskites[130] display insulating antiferromagnetism; rare-earth-based and hole-doped perovskite manganites[133] display metallic ferromagnetism; and transition metal-based spinels[131,134,135] and hexaferrites[136] display insulating ferrimagnetism. Most importantly, the multi-principal occupancy of HEOs leads to local bond diversities, which give rise to several competing clusters of exchange interactions. These interactions may include super-exchange antiferromagnetic and/or ferromagnetic or double-exchange ferromagnetic interactions, revealing themselves through magneto-electronic phase separation within a single-phase structure. This phase separation leads to phenomena such as intrinsic exchange bias[130,137] and colossal magnetoresistance[133]. The degree and nature of magneto-electronic phase separation can be engineered by compositional design[137]. These findings highlight the potential for the high-entropy approach to achieve new magneto-electronic properties, further customizable through composition changes[132,135,138], charge doping[133,139] or substrate-induced epitaxial straining[134,140].

Altogether, several different properties can be altered by the application of the high-entropy concept, with important ramifications for electronic applications (Fig. 4).

## Future research directions

Ionic HEMs have only been studied for a few years, but they hold considerable promise as functional materials. Various methods can be

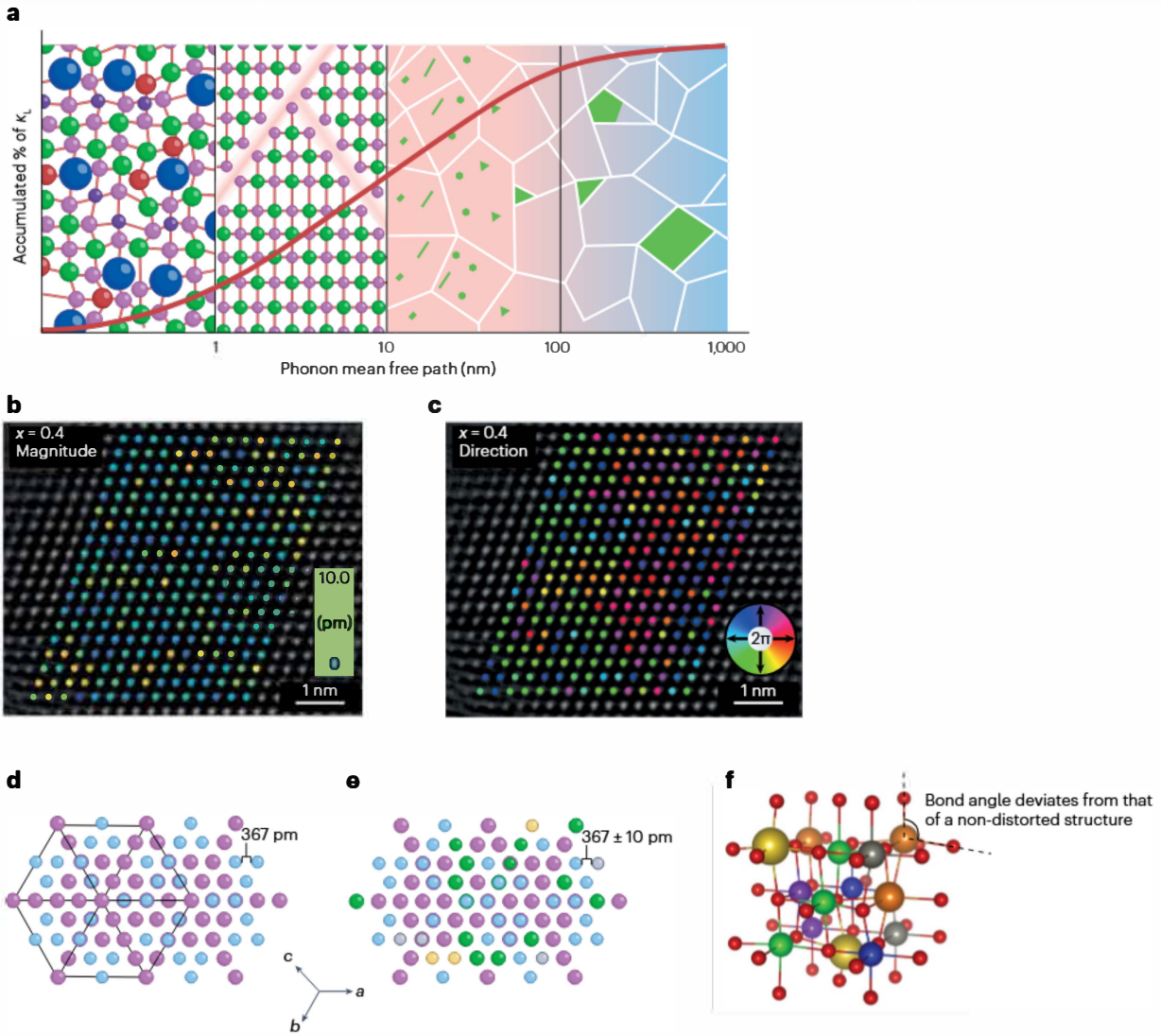


**Fig. 4 | Different effects emerging from the high-entropy concept and how they affect electronic applications. a**, Thermal conductivity versus phonon mean free path in different hierarchical structures. Accumulated percentage of $\kappa_L$ describes the accumulation function of the lattice thermal conductivity. The stronger the disorder, the shorter the free path and the lower the thermal conductivity. **b**, Magnitude of lattice distortion in a high-entropy $Bi_2Ti_2O_7$-type pyrochlore phase [$(Bi_{3.25}La_{0.75})(Ti_{1.8}Zr_{0.4}Hf_{0.4}Sn_{0.4})O_{12}$]. **c**, Displacement directions for the sample in **b**. **d**,**e**, Schematic structures of the $Bi_2Ti_2O_7$ pyrochlore phase (part **d**) and $(Bi_{3.25}La_{0.75})(Ti_{1.8}Zr_{0.4}Hf_{0.4}Sn_{0.4})O_{12}$ (part **e**). According to the measurements in parts **b** and **c**, the distances may vary up to 10 pm from the 367 pm of the ideal structure, corresponding to about 2.7%. **f**, Illustration of bond angles in a distorted lattice. Part **a** reprinted from ref. 113, CC BY 4.0. Parts **b** and **c** reprinted from ref. 7, Springer Nature Limited.

used for their preparation, resulting in different morphologies, for example powder versus film. Although this Perspective focuses mainly on energy and electronic applications, the unique characteristics of HEMs allow for versatile property tailoring (Supplementary Table 1). Therefore, HEMs are likely to find uses in a broad range of applications beyond those discussed here.

## Role of defects

The diversity of the compositional space of HEMs can be further expanded, as is typical in materials development, by the incorporation of defects. Defects (including point defects such as vacancies and interstitials, line defects such as dislocations, interfaces such as grain boundaries and surfaces, and 3D defects such as second-phase particles and pores) can serve as microstructural design elements for creating new materials and enhancing their properties. Defects are ubiquitous in materials used in modern applications, and an understanding of defects is essential to engineer desired properties, such as mechanical strength, magnetic coercivity, catalytic activity, or combined properties such as concomitant electrical conductivity and mechanical strength.

Although the use of defects as design elements to modify and optimize properties has not been fully explored in HEMs, the possibilities are vast. This lack of focus on defect engineering for HEMs is due to the

novelty of the field and the complexity of interactions between defects and the intricate chemical environment, which presents challenges for analytical techniques and simulations. For MoNbTaVW alloys, Schottky defects emerge as the preferred intrinsic defects, with a formation energy of (3.48 ± 0.27) eV per atom[141–143]. Because of the higher energy compared with the average vacancy formation energy in pure tungsten, a lower concentration of vacancies can be expected in the alloy under equilibrium conditions. Notably, interstitials in this compound show almost barrier-free migration even beyond the nearest-neighbour positions. This characteristic suggests a higher likelihood of irradiation damage annihilation, underscoring the suitability of such alloys in nuclear and fusion reactor applications.

Although we have discussed the role of point defects, such as vacancies, introduced by the doping of HEMs with cations or anions of varying valence, the potential for defect engineering is more extensive. The interactions of defects, such as dislocations and grain boundaries, with the complex composition of HEMs can lead to segregation effects, altering the properties of the material, and can lead to properties such as dislocation pinning or radiation damage healing[144,145]. The selective insertion or alteration of elemental stoichiometry can also substantially influence the formation and size of grains. The correlation between certain mechanical properties of materials and grain sizes, a phenomenon well established as the Hall–Petch effect, offers a means to finely adjust material hardness by carefully selecting elements and composition ratios. As a result, these tailored materials can serve as protective coatings in aerospace, the tool industry and the construction sector.

A new avenue for HEM modification would be to decrease the grain size to obtain a large volume fraction of grain boundaries. The effect of grain size on the catalytic activity of HEMs, from high-entropy clusters containing only a limited number of atoms to nanoparticles and micrometre-sized particles, needs to be studied systematically. Porous assemblies of (nano)particles made from HEMs are of interest, with pore size and distribution as design elements for property modification. Furthermore, (nano)composite-type structures consisting of two or more distinct solid phases, at least one of which is an HEM, are complementary to the use of defects as design elements in materials.

The development and understanding of HEMs is still in its early stages. Research on HEAs is more advanced, and initial efforts have been made to study the role of defects in structural and functional properties, but there are still extensive opportunities to understand various types of defects and the complex chemical environment. Although defect chemistry in HECs remains relatively unexplored, studies involving HEOs are promising. For example, the introduction of defects in HEOs has been found to enhance catalytic activities, diffusion properties and electrical behaviour in highly defective spinels such as $(CrMnFeCoNi)_3O_4$ (OER) or in a holey lamellar (CoNiCuMgZn)O catalyst (oxidation of benzyl alcohol)[74,146,147]. Several studies suggest that the formation of oxygen defects in HEOs improves catalytic performance, but the observed improvements might also be attributable to surface modifications. It thus remains uncertain whether the targeted formation of defects, specifically oxygen defects, is the sole determining factor. Nevertheless, the investigations hold promise for future research, not only in HEAs but also in HECs.

## High-throughput synthesis and modelling

A practical challenge in the development of HEMs is their chemical complexity, which complicates the identification of the most promising composition and stoichiometry for a specific property or application. However, high-throughput synthesis and characterization techniques can limit the number of experiments required[148]. These techniques allow for the simultaneous preparation of hundreds of different samples and the automation or parallel performance of characterization procedures, generating vast amounts of data. Ideally, characterization is performed in parallel, as sequential measurements on high-throughput synthesized samples would impede the process. Nevertheless, it is also necessary to first narrow down the chemical parameter space for this kind of screening.

The calculation of properties is a challenge, owing to the lack of thorough structural information and the numerous elements involved. Predictive calculations become too complex for large unit cells, and defining 'small' unit cells leads to superstructures that strongly reduce $\Delta S_{config}$, leading to false results. In the pursuit of desired material properties, the combination of high-throughput synthesis and computational/modelling engineering has emerged as a powerful tool. By using quantum mechanical and thermodynamic calculations alongside database construction and intelligent data analysis techniques, such as the CALPHAD (calculated phase diagram) method, researchers can explore the wide realm of low-, medium- and high-entropy materials[149,150]. Although calculations for alloy systems with dominant elements have been established as reliable and are widely used in the metal industry, caution must be taken when extrapolating to systems lacking a dominant element, as is the case for HEMs. The number and types of predicted phases in HEMs are often reliable, but transformation temperatures, volume fractions and phase compositions demand meticulous scrutiny because of their inherent inaccuracies[9,151,152].

Preliminary experiments attempted to use machine-learning approaches to analyse material libraries, focusing on identifying single-phase structures[153]. However, because of the unavailability of diffraction patterns, additional patterns had to be simulated to establish a foundation for prediction[153]. Automated high-throughput laboratories, preferably with artificial-intelligence-assisted evaluation of material properties, seem the best option for HEM research and development in the future. Prediction of microstructures and cocktail effects, as well as of their impact on the mechanical properties of HEMs, remains an important challenge. The vast chemical parameter space renders precise composition and property predictions nearly impossible. The creation of extensive datasets through high-throughput synthesis and characterization coupled with subsequent machine-learning approaches offers a promising solution to this challenge. These datasets serve as effective training resources for machine-learning models, enabling the predictions of desirable compositions with specific properties or functionalities. These generative predictions in turn can be used in a feedback loop, guiding subsequent high-throughput synthesis using the proposed parameters.

Numerous studies have already explored the integration of high-throughput methods with machine learning and simulation studies. Specifically, investigations into electrochemical energy storage, catalysis and HEAs have yielded insights into how to process, characterize and test HEMs for different applications using high-throughput methods[154–160]. The parameter space governing these systems is virtually boundless, and simulations often deviate from experimental data[161,162]. However, by generating experimental datasets using high-throughput methods, computer-aided synthesis strategies can be refined, leading to predictions that are more accurate. Self-driving laboratories are currently under discussion for various classes of materials. The complexity of HEMs coupled with the numerous available adjustments makes them ideal model systems for such development.

In addition to the HECs discussed in this Perspective, many more materials are expected to enter the realm of HEMs. MOFs and MXenes are examples of materials that have recently been adapted to the high-entropy concept[163,164]. Owing to their unique structure and possibilities, many new applications can be addressed. With an often highly porous, well-ordered structure and large distance between the metal ions, high-entropy MOFs can be used, for example, in electrochemical energy storage or sensor applications, whereas layer-structured high-entropy MXenes seem to be promising electrode and sensing materials. The versatility and infinite chemical and design space of HEMs make them a fascinating class of advanced materials with great potential for discoveries and technical applications.

## References


1. Cantor, B., Chang, I. T. H., Knight, P. & Vincent, A. J. B. Microstructural development in equiatomic multicomponent alloys. *Mater. Sci. Eng. A* **375–377**, 213–218 (2004).
2. Yeh, J.-W. et al. Nanostructured high-entropy alloys with multiple principal elements: novel alloy design concepts and outcomes. *Adv. Eng. Mater.* **6**, 299–303 (2004).
3. Rost, C. M. et al. Entropy-stabilized oxides. *Nat. Commun.* **6**, 8485 (2015).
4. George, E. P., Raabe, D. & Ritchie, R. O. High-entropy alloys. *Nat. Rev. Mater.* **4**, 515–534 (2019).
5. Oses, C., Toher, C. & Curtarolo, S. High-entropy ceramics. *Nat. Rev. Mater.* **5**, 295–309 (2020).
6. Brahlek, M. et al. What is in a name: defining 'high entropy' oxides. *Apl. Mater.* **10**, 110902 (2022).
7. Yang, B. et al. High-entropy enhanced capacitive energy storage. *Nat. Mater.* **21**, 1074–1080 (2022).
8. Aamlid, S. S., Oudah, M., Rottler, J. & Hallas, A. M. Understanding the role of entropy in high entropy oxides. *J. Am. Chem. Soc.* **145**, 5991–6006 (2023).
9. Miracle, D. B. & Senkov, O. N. A critical review of high entropy alloys and related concepts. *Acta Mater.* **122**, 448–511 (2017).
10. Spurling, R. J., Lass, E. A., Wang, X. & Page, K. Entropy-driven phase transitions in complex ceramic oxides. *Phys. Rev. Mater.* **6**, 090301 (2022).
11. Ma, D., Grabowski, B., Körmann, F., Neugebauer, J. & Raabe, D. Ab initio thermodynamics of the CoCrFeMnNi high entropy alloy: importance of entropy contributions beyond the configurational one. *Acta Mater.* **100**, 90–97 (2015).
12. Körmann, F., Ikeda, Y., Grabowski, B. & Sluiter, M. H. F. Phonon broadening in high entropy alloys. *npj Comput. Mater.* **3**, 1–9 (2017).
13. Chang, C.-C. et al. Lattice distortion or cocktail effect dominates the performance of tantalum-based high-entropy nitride coatings. *Appl. Surf. Sci.* **577**, 151894 (2022).
14. Braun, J. L. et al. Charge-induced disorder controls the thermal conductivity of entropy-stabilized oxides. *Adv. Mater.* **30**, 1805004 (2018).
15. Ning, Y. et al. Achieving high energy storage properties in perovskite oxide via high-entropy design. *Ceram. Int.* **49**, 12214–12223 (2023).
16. Bérardan, D., Franger, S., Meena, A. K. & Dragoe, N. Room temperature lithium superionic conductivity in high entropy oxides. *J. Mater. Chem. A* **4**, 9536–9541 (2016).
17. Xiang, H. et al. High-entropy ceramics: present status, challenges, and a look forward. *J. Adv. Ceram.* **10**, 385–441 (2021).
18. Wang, J. et al. P2-type layered high-entropy oxides as sodium-ion cathode materials. *Mater. Futur.* **1**, 035104 (2022).
19. Zhang, R. et al. Compositionally complex doping for zero-strain zero-cobalt layered cathodes. *Nature* **610**, 67–73 (2022).
20. Zhao, C., Ding, F., Lu, Y., Chen, L. & Hu, Y. High-entropy layered oxide cathodes for sodium-ion batteries. *Angew. Chem. Int. Ed.* **59**, 264–269 (2020).
21. Fu, F. et al. Entropy and crystal-facet modulation of P2-type layered cathodes for long-lasting sodium-based batteries. *Nat. Commun.* **13**, 2826 (2022).
22. Ding, F. et al. Using high-entropy configuration strategy to design na-ion layered oxide cathodes with superior electrochemical performance and thermal stability. *J. Am. Chem. Soc.* **144**, 8286–8295 (2022).
23. Ma, Y. et al. High-entropy energy materials: challenges and new opportunities. *Energy Environ. Sci.* **14**, 2883–2905 (2021).
24. Amiri, A. & Shahbazian-Yassar, R. Recent progress of high-entropy materials for energy storage and conversion. *J. Mater. Chem. A* **9**, 782–823 (2021).
25. Lin, L. et al. High-entropy sulfides as electrode materials for Li-ion batteries. *Adv. Energy Mater.* **12**, 2103090 (2022).
26. Sarkar, A. et al. High entropy oxides for reversible energy storage. *Nat. Commun.* **9**, 3400 (2018).
27. Cui, Y. et al. High entropy fluorides as conversion cathodes with tailorable electrochemical performance. *J. Energy Chem.* **72**, 342–351 (2022).
28. Petrovičová, B. et al. High-entropy spinel oxides produced via sol-gel and electrospinning and their evaluation as anodes in Li-ion batteries. *Appl. Sci.* **12**, 5965 (2022).
29. Triolo, C., Xu, W., Petrovičová, B., Pinna, N. & Santangelo, S. Evaluation of entropy-stabilized $(Mg_{0.2}Co_{0.2}Ni_{0.2}Cu_{0.2}Zn_{0.2})O$ oxides produced via solvothermal method or electrospinning as anodes in lithium-ion batteries. *Adv. Funct. Mater.* **32**, 2202892 (2022).
30. Wang, K. et al. Synergy of cations in high entropy oxide lithium ion battery anode. *Nat. Commun.* **14**, 1487 (2023).
31. Wang, Q. et al. Multi-anionic and -cationic compounds: new high entropy materials for advanced Li-ion batteries. *Energy Environ. Sci.* **12**, 2433–2442 (2019).
32. Lun, Z. et al. Cation-disordered rocksalt-type high-entropy cathodes for Li-ion batteries. *Nat. Mater.* **20**, 214–221 (2021).
33. Ma, Y. et al. Resolving the role of configurational entropy in improving cycling performance of multicomponent hexacyanoferrate cathodes for sodium-ion batteries. *Adv. Funct. Mater.* **32**, 2202372 (2022).
34. Ma, Y. et al. High-entropy metal–organic frameworks for highly reversible sodium storage. *Adv. Mater.* **33**, 2101342 (2021).
35. Du, M. et al. High-entropy prussian blue analogues and their oxide family as sulfur hosts for lithium–sulfur batteries. *Angew. Chem.* **134**, e202209350 (2022).
36. Xing, J., Zhang, Y., Jin, Y. & Jin, Q. Active cation-integration high-entropy Prussian blue analogues cathodes for efficient Zn storage. *Nano Res.* **16**, 2486–2494 (2023).
37. Varzi, A., Mattarozzi, L., Cattarin, S., Guerriero, P. & Passerini, S. 3D porous Cu–Zn alloys as alternative anode materials for Li-Ion batteries with superior low *T* performance. *Adv. Energy Mater.* **8**, 1701706 (2018).
38. Wei, Y. et al. Embedding the high entropy alloy nanoparticles into carbon matrix toward high performance Li-ion batteries. *J. Alloy. Compd.* **938**, 168610 (2023).
39. Osenciat, N. et al. Charge compensation mechanisms in Li-substituted high-entropy oxides and influence on Li superionic conductivity. *J. Am. Ceram. Soc.* **102**, 6156–6162 (2019).
40. Biesuz, M. et al. Ni-free high-entropy rock salt oxides with Li superionic conductivity. *J. Mater. Chem. A* **10**, 23603–23616 (2022).
41. Grzesik, Z. et al. Defect structure and transport properties in (Co,Cu,Mg,Ni,Zn)O high entropy oxide. *J. Eur. Ceram. Soc.* **39**, 4292–4298 (2019).
42. Zeng, Y. et al. High-entropy mechanism to boost ionic conductivity. *Science* **378**, 1320–1324 (2022).
43. Stockham, M. P., Dong, B. & Slater, P. R. High entropy lithium garnets — testing the compositional flexibility of the lithium garnet system. *J. Solid. State Chem.* **308**, 122944 (2022).
44. Kuo, C.-H. et al. A novel garnet-type high-entropy oxide as air-stable solid electrolyte for Li-ion batteries. *Apl. Mater.* **10**, 121104 (2022).
45. Sastre, J. et al. Lithium garnet $Li_7La_3Zr_2O_{12}$ electrolyte for all-solid-state batteries: closing the gap between bulk and thin film Li-ion conductivities. *Adv. Mater. Interfaces* **7**, 2000425 (2020).
46. Lin, J. et al. A high-entropy multicationic substituted lithium argyrodite superionic solid electrolyte. *ACS Mater. Lett.* **4**, 2187–2194 (2022).
47. Strauss, F. et al. High-entropy polyanionic lithium superionic conductors. *ACS Mater. Lett.* **4**, 418–423 (2022).
48. Możdzierz, M. et al. Mixed ionic-electronic transport in the high-entropy $(Co,Cu,Mg,Ni,Zn)_{1-x}Li_xO$ oxides. *Acta Mater.* **208**, 116735 (2021).
49. Hsu, S.-H. et al. An earth-abundant catalyst-based seawater photoelectrolysis system with 17.9% solar-to-hydrogen efficiency. *Adv. Mater.* **30**, 1707261 (2018).
50. Guan, J., Bai, X. & Tang, T. Recent progress and prospect of carbon-free single-site catalysts for the hydrogen and oxygen evolution reactions. *Nano Res.* **15**, 818–837 (2022).
51. Lee, Y., Suntivich, J., May, K. J., Perry, E. E. & Shao-Horn, Y. Synthesis and activities of rutile $IrO_2$ and $RuO_2$ nanoparticles for oxygen evolution in acid and alkaline solutions. *J. Phys. Chem. Lett.* **3**, 399–404 (2012).
52. Liu, J. et al. NiO as a bifunctional promoter for $RuO_2$ toward superior overall water splitting. *Small* **14**, 1704073 (2018).
53. Koo, J. Y. et al. Suppression of cation segregation in $(La,Sr)CoO_{3-\delta}$ by elastic energy minimization. *ACS Appl. Mater. Interfaces* **10**, 8057–8065 (2018).
54. Fu, M., Ma, X., Zhao, K., Li, X. & Su, D. High-entropy materials for energy-related applications. *iScience* **24**, 102177 (2021).
55. Sun, Y. & Dai, S. High-entropy materials for catalysis: a new frontier. *Sci. Adv.* **7**, eabg1600 (2021).
56. Tsai, C.-F., Wu, P.-W., Lin, P., Chao, C.-G. & Yeh, K.-Y. Sputter deposition of multi-element nanoparticles as electrocatalysts for methanol oxidation. *Jpn. J. Appl. Phys.* **47**, 5755–5761 (2008).
57. Tsai, C.-F., Yeh, K.-Y., Wu, P.-W., Hsieh, Y.-F. & Lin, P. Effect of platinum present in multi-element nanoparticles on methanol oxidation. *J. Alloy. Compd.* **478**, 868–871 (2009).
58. Yao, Y. et al. Carbothermal shock synthesis of high-entropy-alloy nanoparticles. *Science* **359**, 1489–1494 (2018).
59. Yao, Y. et al. Computationally aided, entropy-driven synthesis of highly efficient and durable multi-elemental alloy catalysts. *Sci. Adv.* **6**, eaaz0510 (2020).
60. Xie, P. et al. Highly efficient decomposition of ammonia using high-entropy alloy catalysts. *Nat. Commun.* **10**, 4011 (2019).
61. Ding, Z. et al. High entropy intermetallic–oxide core–shell nanostructure as superb oxygen evolution reaction catalyst. *Adv. Sustain. Syst.* **4**, 1900105 (2020).
62. Jin, Z. et al. Nanoporous Al-Ni-Co-Ir-Mo high-entropy alloy for record-high water splitting activity in acidic environments. *Small* **15**, 1904180 (2019).

63. Schweidler, S. et al. Synthesis of perovskite-type high-entropy oxides as potential candidates for oxygen evolution. *Front. Energy Res.* **10**, 983979 (2022).
64. Wang, T., Chen, H., Yang, Z., Liang, J. & Dai, S. High-entropy perovskite fluorides: a new platform for oxygen evolution catalysis. *J. Am. Chem. Soc.* **142**, 4550–4554 (2020).
65. Stenzel, D. et al. High-entropy spinel-structure oxides as oxygen evolution reaction electrocatalyst. *Front. Energy Res.* **10**, 942314 (2022).
66. Nguyen, T. X., Su, Y., Lin, C. & Ting, J. Self-reconstruction of sulfate-containing high entropy sulfide for exceptionally high-performance oxygen evolution reaction electrocatalyst. *Adv. Funct. Mater.* **31**, 2106229 (2021).
67. Sun, Z. et al. High entropy spinel-structure oxide for electrochemical application. *Chem. Eng. J.* **431**, 133448 (2022).
68. Zhai, S. et al. The use of poly-cation oxides to lower the temperature of two-step thermochemical water splitting. *Energy Environ. Sci.* **11**, 2172–2178 (2018).
69. Qiu, H.-J. et al. Noble metal-free nanoporous high-entropy alloys as highly efficient electrocatalysts for oxygen evolution reaction. *ACS Mater. Lett.* **1**, 526–533 (2019).
70. Einert, M. et al. Mesoporous high-entropy oxide thin films: electrocatalytic water oxidation on high-surface-area spinel $(Cr_{0.2}Mn_{0.2}Fe_{0.2}Co_{0.2}Ni_{0.2})_3O_4$ electrodes. *ACS Appl. Energy Mater.* **5**, 717–730 (2022).
71. Nguyen, T. X., Liao, Y.-C., Lin, C.-C., Su, Y.-H. & Ting, J.-M. Advanced high entropy perovskite oxide electrocatalyst for oxygen evolution reaction. *Adv. Funct. Mater.* **31**, 2101632 (2021).
72. Duan, C. et al. Nanosized high entropy spinel oxide $(FeCoNiCrMn)_3O_4$ as a highly active and ultra-stable electrocatalyst for the oxygen evolution reaction. *Sustain. Energy Fuels* **6**, 1479–1488 (2022).
73. Dąbrowa, J. et al. Formation of solid solutions and physicochemical properties of the high-entropy $Ln_{1-x}Sr_x(Co,Cr,Fe,Mn,Ni)O_{3-\delta}$ (Ln = La, Pr, Nd, Sm or Gd) perovskites. *Materials* **14**, 5264 (2021).
74. Triolo, C. et al. Evaluation of electrospun spinel-type high-entropy $(Cr_{0.2}Mn_{0.2}Fe_{0.2}Co_{0.2}Ni_{0.2})_3O_4$, $(Cr_{0.2}Mn_{0.2}Fe_{0.2}Co_{0.2}Zn_{0.2})_3O_4$ and $(Cr_{0.2}Mn_{0.2}Fe_{0.2}Ni_{0.2}Zn_{0.2})_3O_4$ oxide nanofibers as electrocatalysts for oxygen evolution in alkaline medium. *Energy Adv.* **2**, 667–678 (2023).
75. Li, X. et al. High entropy materials based electrocatalysts for water splitting: synthesis strategies, catalytic mechanisms, and prospects. *Nano Res.* https://doi.org/10.1007/s12274-022-5207-4 (2022).
76. Zhang, G. et al. High entropy alloy as a highly active and stable electrocatalyst for hydrogen evolution reaction. *Electrochim. Acta* **279**, 19–23 (2018).
77. Löffler, T. et al. Toward a paradigm shift in electrocatalysis using complex solid solution nanoparticles. *ACS Energy Lett.* **4**, 1206–1214 (2019).
78. Li, J., Liu, Y., Chen, H., Zhang, Z. & Zou, X. Design of a multilayered oxygen-evolution electrode with high catalytic activity and corrosion resistance for saline water splitting. *Adv. Funct. Mater.* **31**, 2101820 (2021).
79. Tong, W. et al. Electrolysis of low-grade and saline surface water. *Nat. Energy* **5**, 367–377 (2020).
80. Kuang, Y. et al. Solar-driven, highly sustained splitting of seawater into hydrogen and oxygen fuels. *Proc. Natl Acad. Sci. USA* **116**, 6624–6629 (2019).
81. Vos, J. G., Wezendonk, T. A., Jeremiasse, A. W. & Koper, M. T. M. $MnO_x/IrO_x$ as selective oxygen evolution electrocatalyst in acidic chloride solution. *J. Am. Chem. Soc.* **140**, 10270–10281 (2018).
82. Bennett, J. Electrodes for generation of hydrogen and oxygen from seawater. *Int. J. Hydrog. Energy* **5**, 401–408 (1980).
83. Arnold, S., Wang, L. & Presser, V. Dual-use of seawater batteries for energy storage and water desalination. *Small* **18**, 2107913 (2022).
84. Hong, J., Cho, K.-H., Presser, V. & Su, X. Recent advances in wastewater treatment using semiconductor photocatalysts. *Curr. Opin. Green Sustain. Chem.* **36**, 100644 (2022).
85. Srimuk, P., Su, X., Yoon, J., Aurbach, D. & Presser, V. Charge-transfer materials for electrochemical water desalination, ion separation and the recovery of elements. *Nat. Rev. Mater.* **5**, 517–538 (2020).
86. Wang, L., Zhang, Y., Moh, K. & Presser, V. From capacitive deionization to desalination batteries and desalination fuel cells. *Curr. Opin. Electrochem.* **29**, 100758 (2021).
87. Löffler, T., Ludwig, A., Rossmeisl, J. & Schuhmann, W. What makes high-entropy alloys exceptional electrocatalysts? *Angew. Chem. Int. Ed.* **60**, 26894–26903 (2021).
88. Zhang, Y. et al. *In situ* coupling of Ag nanoparticles with high-entropy oxides as highly stable bifunctional catalysts for wearable Zn–Ag/Zn–air hybrid batteries. *Nanoscale* **13**, 16164–16171 (2021).
89. Baiutti, F. et al. A high-entropy manganite in an ordered nanocomposite for long-term application in solid oxide cells. *Nat. Commun.* **12**, 2660 (2021).
90. Jin, Z. et al. Eight-component nanoporous high-entropy oxides with low Ru contents as high-performance bifunctional catalysts in Zn–air batteries. *Small* **18**, 2107207 (2022).
91. Jin, Z. et al. A fourteen-component high-entropy alloy@oxide bifunctional electrocatalyst with a record-low $\Delta E$ of 0.61 V for highly reversible Zn–air batteries. *Chem. Sci.* **13**, 12056–12064 (2022).
92. Yu, T., Xu, H., Jin, Z., Zhang, Y. & Qiu, H.-J. Noble metal-free high-entropy oxide/Co–N–C bifunctional electrocatalyst enables highly reversible and durable Zn-air batteries. *Appl. Surf. Sci.* **610**, 155624 (2023).
93. Guo, R. & He, T. High-entropy perovskite electrolyte for protonic ceramic fuel cells operating below 600 °C. *ACS Mater. Lett.* **4**, 1646–1652 (2022).
94. Bersuker, G., Zeitzoff, P., Brown, G. & Huff, H. R. Dielectrics for future transistors. *Mater. Today* **7**, 26–33 (2004).
95. Kim, L., Jung, D., Kim, J., Kim, Y. S. & Lee, J. Strain manipulation in $BaTiO_3/SrTiO_3$ artificial lattice toward high dielectric constant and its nonlinearity. *Appl. Phys. Lett.* **82**, 2118–2120 (2003).
96. Sharma, Y. et al. High entropy oxide relaxor ferroelectrics. *ACS Appl. Mater. Interfaces* **14**, 11962–11970 (2022).
97. Zhang, X. et al. Dielectric properties of novel high-entropy $(La_{0.2}Li_{0.2}Ba_{0.2}Sr_{0.2}Ca_{0.2})Nb_2O_{6-\delta}$ tungsten bronze ceramics. *J. Mater. Sci.* **57**, 15901–15912 (2022).
98. Zhou, J., Li, P., Zhang, X., Yan, J. & Qi, X. Effect of configurational entropy on dielectric properties of high-entropy perovskite oxides $(Ce_{0.5},K_{0.5})_x[(Bi_{0.5},Na_{0.5})_{0.25}Ba_{0.25}Sr_{0.25}Ca_{0.25}]_{1-x}TiO_3$. *J. Mater. Sci. Mater. Electron.* **33**, 20721–20730 (2022).
99. Ning, Y. et al. Enhanced capacitive energy storage and dielectric temperature stability of A-site disordered high-entropy perovskite oxides. *J. Mater. Sci. Technol.* **145**, 66–73 (2023).
100. Zhou, S. et al. Dielectric temperature stability and energy storage performance of NBT-based ceramics by introducing high-entropy oxide. *J. Am. Ceram. Soc.* **105**, 4796–4804 (2022).
101. Li, H. et al. High-entropy oxides: advanced research on electrical properties. *Coatings* **11**, 628 (2021).
102. Talluri, B., Aparna, M. L., Sreenivasulu, N., Bhattacharya, S. S. & Thomas, T. High entropy spinel metal oxide $(CoCrFeMnNi)_3O_4$ nanoparticles as a high-performance supercapacitor electrode material. *J. Energy Storage* **42**, 103004 (2021).
103. Xuan, Y., Lin, H. C., Ye, P. D. & Wilk, G. D. Capacitance-voltage studies on enhancement-mode InGaAs metal–oxide–semiconductor field-effect transistor using atomic-layer-deposited $Al_2O_3$ gate dielectric. *Appl. Phys. Lett.* **88**, 263518 (2006).
104. Feng, X., Marques, G. C., Rasheed, F., Tahoori, M. B. & Aghassi-Hagmann, J. Nonquasi-static capacitance modeling and characterization for printed inorganic electrolyte-gated transistors in logic gates. *IEEE Trans. Electron. Devices* **66**, 5272–5277 (2019).
105. Kim, S. H. et al. Electrolyte-gated transistors for organic and printed electronics. *Adv. Mater.* **25**, 1822–1846 (2013).
106. Yang, B. et al. High-entropy design for dielectric materials: status, challenges, and beyond. *J. Appl. Phys.* **133**, 110904 (2023).
107. Zhang, P. et al. High-entropy $(Ca_{0.2}Sr_{0.2}Ba_{0.2}La_{0.2}Pb_{0.2})TiO_3$ perovskite ceramics with A-site short-range disorder for thermoelectric applications. *J. Mater. Sci. Technol.* **97**, 182–189 (2022).
108. Ma, Z. et al. High thermoelectric performance and low lattice thermal conductivity in lattice-distorted high-entropy semiconductors $AgMnSn_{1-x}Pb_xSbTe_4$. *Chem. Mater.* **34**, 8959–8967 (2022).
109. Rost, C. M. et al. Electron and phonon thermal conductivity in high entropy carbides with variable carbon content. *Acta Mater.* **196**, 231–239 (2020).
110. Zhang, R.-Z., Gucci, F., Zhu, H., Chen, K. & Reece, M. J. Data-driven design of ecofriendly thermoelectric high-entropy sulfides. *Inorg. Chem.* **57**, 13027–13033 (2018).
111. Fan, L. et al. A novel $MnCoNiCuZnO_5$ complex-phase ceramic for negative temperature coefficient thermistors. *Mater. Sci. Semicond. Process.* **142**, 106489 (2022).
112. Shi, Z. et al. A-site deficiency improved the thermoelectric performance of high-entropy perovskite manganite-based ceramics. *J. Mater. Chem. C* https://doi.org/10.1039/D2TC02952A (2022).
113. Jiang, B. et al. Entropy engineering promotes thermoelectric performance in p-type chalcogenides. *Nat. Commun.* **12**, 3234 (2021).
114. Jiang, B. et al. High-entropy-stabilized chalcogenides with high thermoelectric performance. *Science* **371**, 830–834 (2021).
115. Wright, A. J. et al. Size disorder as a descriptor for predicting reduced thermal conductivity in medium- and high-entropy pyrochlore oxides. *Scr. Mater.* **181**, 76–81 (2020).
116. Lim, M. et al. Influence of mass and charge disorder on the phonon thermal conductivity of entropy stabilized oxides determined by molecular dynamics simulations. *J. Appl. Phys.* **125**, 055105 (2019).
117. Franz, R. & Wiedemann, G. Ueber die Wärme-Leitungsfähigkeit der Metalle. *Ann. Phys. Chem.* **165**, 497–531 (1853).
118. Zheng, Y. et al. Electrical and thermal transport behaviours of high-entropy perovskite thermoelectric oxides. *J. Adv. Ceram.* **10**, 377–384 (2021).
119. Banerjee, R. et al. High-entropy perovskites: an emergent class of oxide thermoelectrics with ultralow thermal conductivity. *ACS Sustain. Chem. Eng.* **8**, 17022–17032 (2020).
120. Luo, Y. et al. High thermoelectric performance in the new cubic semiconductor $AgSnSbSe_3$ by high-entropy engineering. *J. Am. Chem. Soc.* **142**, 15187–15198 (2020).
121. Deng, Z. et al. Semiconducting high-entropy chalcogenide alloys with ambi-ionic entropy stabilization and ambipolar doping. *Chem. Mater.* **32**, 6070–6077 (2020).
122. Mikuła, A. et al. Search for mid- and high-entropy transition-metal chalcogenides — investigating the pentlandite structure. *Dalton Trans.* **50**, 9560–9573 (2021).
123. Krawczyk, P. A. et al. High-entropy perovskites as multifunctional metal oxide semiconductors: synthesis and characterization of $(Gd_{0.2}Nd_{0.2}La_{0.2}Sm_{0.2}Y_{0.2})CoO_3$. *ACS Appl. Electron. Mater.* **2**, 3211–3220 (2020).
124. Liang, Y., Luo, B., Dong, H. & Wang, D. Electronic structure and transport properties of sol-gel-derived high-entropy $Ba(Zr_{0.2}Sn_{0.2}Ti_{0.2}Hf_{0.2}Nb_{0.2})O_3$ thin films. *Ceram. Int.* **47**, 20196–20200 (2021).
125. Usharani, N. J., Sanghavi, H. & Bhattacharya, S. S. Factors influencing phase formation and band gap studies of a novel multicomponent high entropy $(Co,Cu,Mg,Ni,Zn)_2TiO_4$ orthotitanate spinel. *J. Alloy. Compd.* **888**, 161390 (2021).
126. Mazza, A. R. et al. Searching for superconductivity in high entropy oxide Ruddlesden–Popper cuprate films. *J. Vac. Sci. Technol. A* **40**, 013404 (2022).

127. Sarkar, A., Kruk, R. & Hahn, H. Magnetic properties of high entropy oxides. *Dalton Trans.* **50**, 1973–1982 (2021).
128. Zhang, J. et al. Long-range antiferromagnetic order in a rocksalt high entropy oxide. *Chem. Mater.* **31**, 3705–3711 (2019).
129. Su, L. et al. Direct observation of elemental fluctuation and oxygen octahedral distortion-dependent charge distribution in high entropy oxides. *Nat. Commun.* **13**, 2358 (2022).
130. Witte, R. et al. High-entropy oxides: an emerging prospect for magnetic rare-earth transition metal perovskites. *Phys. Rev. Mater.* **3**, 034406 (2019).
131. Sarkar, A. et al. Comprehensive investigation of crystallographic, spin-electronic and magnetic structure of $(Co_{0.2}Cr_{0.2}Fe_{0.2}Mn_{0.2}Ni_{0.2})_3O_4$: unraveling the suppression of configuration entropy in high entropy oxides. *Acta Mater.* **226**, 117581 (2022).
132. Jimenez-Segura, M. P. et al. Long-range magnetic ordering in rocksalt-type high-entropy oxides. *Appl. Phys. Lett.* **114**, 122401 (2019).
133. Sarkar, A. et al. High entropy approach to engineer strongly correlated functionalities in manganites. *Adv. Mater*. https://doi.org/10.1002/adma.202207436 (2022).
134. Sharma, Y. et al. Magnetic texture in insulating single crystal high entropy oxide spinel films. *ACS Appl. Mater. Interfaces* **13**, 17971–17977 (2021).
135. Johnstone, G. H. J. et al. Entropy engineering and tunable magnetic order in the spinel high-entropy oxide. *J. Am. Chem. Soc.* **144**, 20590–20600 (2022).
136. Vinnik, D. A. et al. High-entropy oxide phases with magnetoplumbite structure. *Ceram. Int.* **45**, 12942–12948 (2019).
137. Mazza, A. R. et al. Designing magnetism in high entropy oxides. *Adv. Sci.* **9**, 2200391 (2022).
138. Musicó, B. et al. Tunable magnetic ordering through cation selection in entropic spinel oxides. *Phys. Rev. Mater.* **3**, 104416 (2019).
139. Mazza, A. R. et al. Charge doping effects on magnetic properties of single-crystal $La_{1-x}Sr_x(Cr_{0.2}Mn_{0.2}Fe_{0.2}Co_{0.2}Ni_{0.2})O_3$ ($0 \le x \le 0.5$) high-entropy perovskite oxides. *Phys. Rev. B* **104**, 094204 (2021).
140. Sharma, Y. et al. Magnetic anisotropy in single-crystal high-entropy perovskite oxide $La(Cr_{0.2}Mn_{0.2}Fe_{0.2}Co_{0.2}Ni_{0.2})O_3$ films. *Phys. Rev. Mater.* **4**, 014404 (2020).
141. Zhao, S. Role of chemical disorder and local ordering on defect evolution in high-entropy alloys. *Phys. Rev. Mater.* **5**, 103604 (2021).
142. Lin-Vines, A. X. et al. Defect behaviour in the MoNbTaVW high entropy alloy (HEA). *Results Mater.* **15**, 100320 (2022).
143. Pickering, E. J. et al. High-entropy alloys for advanced nuclear applications. *Entropy* **23**, 98 (2021).
144. Aksoy, D. et al. Chemical order transitions within extended interfacial segregation zones in NbMoTaW. *J. Appl. Phys.* **132**, 235302 (2022).
145. McCarthy, M. J. et al. Emergence of near-boundary segregation zones in face-centered cubic multiprincipal element alloys. *Phys. Rev. Mater.* **5**, 113601 (2021).
146. Shu, Y., Bao, J., Yang, S., Duan, X. & Zhang, P. Entropy-stabilized metal-$CeO_x$ solid solutions for catalytic combustion of volatile organic compounds. *AIChE J.* **67**, e17046 (2021).
147. Feng, D. et al. Holey lamellar high-entropy oxide as an ultra-high-activity heterogeneous catalyst for solvent-free aerobic oxidation of benzyl alcohol. *Angew. Chem. Int. Ed.* **59**, 19503–19509 (2020).
148. Wang, Q., Velasco, L., Breitung, B. & Presser, V. High-entropy energy materials in the age of big data: a critical guide to next-generation synthesis and applications. *Adv. Energy Mater.* **11**, 2102355 (2021).
149. Senkov, O. N., Miller, J. D., Miracle, D. B. & Woodward, C. Accelerated exploration of multi-principal element alloys for structural applications. *Calphad* **50**, 32–48 (2015).
150. Senkov, O. N., Miller, J. D., Miracle, D. B. & Woodward, C. Accelerated exploration of multi-principal element alloys with solid solution phases. *Nat. Commun.* **6**, 6529 (2015).
151. Chang, Y. A. et al. Phase diagram calculation: past, present and future. *Prog. Mater. Sci.* **49**, 313–345 (2004).
152. Chou, K.-C. & Austin Chang, Y. A study of ternary geometrical models. *Ber. Bunsenges. Phys. Chem.* **93**, 735–741 (1989).
153. Velasco, L. et al. Phase–property diagrams for multicomponent oxide systems toward materials libraries. *Adv. Mater.* **33**, 2102301 (2021).
154. Kante, M. V. et al. A high-entropy oxide as high-activity electrocatalyst for water oxidation. *ACS Nano* **17**, 5329–5339 (2023).
155. Banko, L. et al. Unravelling composition–activity–stability trends in high entropy alloy electrocatalysts by using a data-guided combinatorial synthesis strategy and computational modeling. *Adv. Energy Mater.* **12**, 2103312 (2022).
156. Ludwig, A., Zarnetta, R., Hamann, S., Savan, A. & Thienhaus, S. Development of multifunctional thin films using high-throughput experimentation methods. *Int. J. Mater. Res.* **99**, 1144–1149 (2008).
157. Li, Z., Ludwig, A., Savan, A., Springer, H. & Raabe, D. Combinatorial metallurgical synthesis and processing of high-entropy alloys. *J. Mater. Res.* **33**, 3156–3169 (2018).
158. Ludwig, A. Discovery of new materials using combinatorial synthesis and high-throughput characterization of thin-film materials libraries combined with computational methods. *npj Comput. Mater.* **5**, 70 (2019).
159. Jia, S., Counsell, J., Adamič, M., Jonderian, A. & McCalla, E. High-throughput design of Na–Fe–Mn–O cathodes for Na-ion batteries. *J. Mater. Chem. A* **10**, 251–265 (2021).
160. Potts, K. P., Grignon, E. & McCalla, E. Accelerated screening of high-energy lithium-ion battery cathodes. *ACS Appl. Energy Mater.* **2**, 8388–8393 (2019).
161. Kumbhakar, M. et al. High-throughput screening of high-entropy fluorite-type oxides as potential candidates for photovoltaic applications. *Adv. Energy Mater.* **13**, 2204337 (2023).
162. Schweidler, S. et al. Synthesis and characterization of high-entropy CrMoNbTaVW thin films using high-throughput methods. *Adv. Eng. Mater.* **25**, 2200870 (2023).
163. Anasori, B. & Gogotsi, Y. MXenes: trends, growth, and future directions. *Graphene 2D Mater.* **7**, 75–79 (2022).
164. Nemani, S. K. et al. High-entropy 2D carbide MXenes: $TiVNbMoC_3$ and $TiVCrMoC_3$. *ACS Nano* **15**, 12815–12825 (2021).
165. Usharani, N. J., Shringi, R., Sanghavi, H., Subramanian, S. & Bhattacharya, S. S. Role of size, alio-/multi-valency and non-stoichiometry in the synthesis of phase-pure high entropy oxide (Co,Cu,Mg,Na,Ni,Zn)O. *Dalton Trans.* **49**, 7123–7132 (2020).
166. Fultz, B. Vibrational thermodynamics of materials. *Prog. Mater. Sci.* **55**, 247–352 (2010).
167. Oh, H. S. et al. Lattice distortions in the FeCoNiCrMn high entropy alloy studied by theory and experiment. *Entropy* **18**, 321 (2016).


## Acknowledgements


Financial support by the Deutsche Forschungsgemeinschaft (DFG, German Research Foundation) is acknowledged by H.H. (HA 1344/45-1), by H.H. and A.S. (HA 1344/43-2), and by L.V. (LV 1111/1-1). L.V., M.B. and H.H. are grateful for the support provided by the DFG (424789449 and SE 1407/4-2). S.S., M.B. and H.H. acknowledge the European Union's Horizon 2020 project EPISTORE with grant agreement no. 101017709. F.S. acknowledges the Federal Ministry of Education and Research (BMBF) for funding within the project MELLi (03XP0447). B.B. thanks the Carl Zeiss Foundation for funding of the KeraSolar project. J.A.-H. acknowledges funding by the DFG under Germany's Excellence Strategy via the Excellence Cluster "3D Matter Made to Order" (EXC-2082/1-390761711). The authors acknowledge the use of ChatGPT for language corrections.


## Author contributions

All authors researched data for the article and wrote the article. T.B. and B.B. reviewed and edited the manuscript before submission.

## Competing interests

The authors declare no competing interests.